HHS Public Access

Author manuscript

J Steroid Biochem Mol Biol. Author manuscript; available in PMC 2023 February 27.

Published in final edited form as:

J Steroid Biochem Mol Biol. 2019 June ; 190: 212–223. doi:10.1016/j.jsbmb.2019.03.022.

Progesterone Receptor Isoform B Expression in Pulmonary Neuroendocrine Cells Decreases Cell Proliferation

Teeranut Asavasupreechar[1], **Ryoko Saito**[2], **Dean P. Edwards**[3], **Hironobu Sasano**[2], **Viroj Boonyaratanakornkit**[1,4,5,*]

[1]Graduate Program in Clinical Biochemistry and Molecular Medicine, Faculty of Allied Health Sciences, Chulalongkorn University, Bangkok, Thailand

[2]Department of Anatomic Pathology, Tohoku University Graduate School of Medicine, Sendai, Japan

[3]Departments of Molecular & Cellular Biology and Pathology & Immunology, Baylor College of Medicine, Houston, USA

[4]Department of Clinical Chemistry, Faculty of Allied Health Sciences, Chulalongkorn University, Bangkok, Thailand.

[5]Age-related Inflammation and Degeneration Research Unit, Chulalongkorn University, Bangkok, Thailand

Abstract

The progesterone receptor (PR) has been reported to play important roles in lung development and function, such as alveolarization, alveolar fluid clearance (AFC) and upper airway dilator muscle activity. In the lung, pulmonary neuroendocrine cells (PNECs) are important in the etiology and progression of lung neuroendocrine tumors (NETs). Women with lung NETs had significantly better survival rates than men, suggesting that sex steroids and their receptors, such as the PR, could be involved in the progression of lung NETs. The PR exists as two major isoforms, PRA and PRB. How the expression of different PR isoforms affects proliferation and the development of lung NETs is not well understood. To determine the role of the PR isoforms in PNECs, we constructed H727 lung NET cell models expressing PRB, PRA, Green Fluorescence Protein (GFP) (control). The expression of PRB significantly inhibited H727 cell proliferation better than that of PRA in the absence of progestin. The expression of the unrelated protein, GFP, had little to no effect on H727 cell proliferation. To better understand the role of the PR isoform in PNECs, we examined PR isoform expression in PNECs in lung tissues. A monoclonal antibody specific to the N-terminus of PRB (250H11 mAb) was developed to specifically recognize PRB, while a monoclonal antibody specific to a common N-terminus epitope present in both PRA and PRB (1294 mAb) was used to detect both PRA and PRB. Using these PR and PRB-specific antibodies, we demonstrated that PR (PRA&PRB) and PRB were expressed in the PNECs of the normal fetal and adult lung, with significantly higher PR expression in the fetal lung. Interestingly, PRB expression in the normal lung was associated with lower cell proliferation than PR expression,

*Corresponding Author Viroj Boonyaratanakornkit, Ph.D., Department of Clinical Chemistry, Faculty of Allied Health Sciences, Chulalongkorn University, 154 Rama I Rd., Wangmai, Pathumwan, Bangkok 10330, Thailand, Viroj.b@chula.ac.th, Tel: +662-218-1081 x 314, Fax: +662-218-1082.

suggesting a distinct role of PRB in the PNECs. A better understanding of the molecular mechanism of PR and PR isoform signaling in lung NET cells may help in developing novel therapeutic strategies that will benefit lung NET patients in the future.

Keywords

Progesterone receptor isoforms A and B; pulmonary neuroendocrine cell; isoform-specific antibody

Introduction

It is well established that sex steroids and their receptors play a key role in the development and homeostasis of endocrine and reproductive tissues. However, little is known about the roles of sex steroids and their receptors in nontraditional endocrine tissues. Recently, several pieces of evidence have suggested that sex steroids may play significant roles in lung development, maturation and the maintenance of normal lung functions. In newborn piglets, treatment with estrogen and progesterone receptor antagonists impairs alveolarization and amiloride-sensitive alveolar fluid clearance (AFC) (1). In the immature rat, the administration of progesterone together with estrogen increases the level of mRNA encoding rat epithelial Na channels (rENaC), a key factor for reabsorbing alveolar fluid (2). Sex steroids have also been shown to be involved in lung maturation. In cultured primary fetal lung epithelial cells, treatment with estradiol in combination with progesterone enhances the expression of VEGF and surfactant proteins (SP)-B and -C (3), which are markers of lung maturation (4). In the normal adult lung, progesterone has been shown to play an important role in respiratory functions. In male and female adult cats, progesterone acts as a respiratory facilitation (5). In male rats, treatment with estrogen and progesterone leads to an increase in tidal volume, a decrease in arterial P_{CO2} and an enhancement of the ventilatory response to CO_2 inhalation (6). Sex steroids mediate their biological functions through their receptors, suggesting that steroid hormone receptors, including the estrogen and progesterone receptor (ER and PR), may play significant roles in lung development and maturation.

The expression of all sex steroid receptors, including the estrogen receptor (ER) and the progesterone receptor (PR), has been found in normal lung tissues (7). In mice, ER and PR mRNA expressions are at the highest levels in the prenatal lung and significantly decrease in the postnatal and adult lung (8). In normal human and rodent lung tissues, the ER and estrogen play important physiological functions in promoting proliferation and alveolar formation during the development and maintenance of pulmonary diffusion capacity, while the androgen receptor (AR) and androgens delay lung maturation (9, 10). PR mRNA has been shown to be expressed in normal lung tissue. PR expression in non-malignant/normal lung tissues was 3-fold higher than that of adenocarcinoma or squamous cell carcinoma (11). The PR was shown to be regulated by progesterone in airway smooth muscle cells (ASMC) (12). Progesterone treatment resulted in an increase in upper airway dilator muscle activity and a significant increase in genioglossus electromyogram (EMGgg) after hormone

replacement therapy in postmenopausal women, protecting them from the development of obstructive sleep apnea (13).

Interestingly, among normal lung cells, pulmonary neuroendocrine cells (PNECs) contribute significantly to overall lung neuroendocrine functions and play a key role in lung development (14). PNECs represent less than 1% of total lung epithelial cells (15) and were more often found during fetal and neonatal development (16, 17) than in adult cells (18). PNECs are amine- and peptide-producing cells (19, 20) and help promote lung branching morphogenesis (21), growth and maturation (22, 23). Transcription factors, such as helix loop helix and notch/notch ligands, have been shown to be involved in the differentiation of neuroendocrine cells in fetal lung epithelium (24). Interestingly, lung neuroendocrine tumors (NETs) often arise from PNECs (25).

Lung NETs are relatively rare but have gained attention in recent years (26, 27). There has been an unexplained but substantial increase in the incidence of lung NETs over the past 30 years (26), with an incident of approximately 0.2 to 2 per 100,000 patients per year (28). Lung NETs account for 1–2% of lung cancers (29) and 25–30% of all NETs (26, 30). According to the 2015 World Health Organization (WHO) classification, there are four types of lung NETs, including typical carcinoid (TC), atypical carcinoid (AC), large cell neuroendocrine carcinoma (LCNEC), and small cell lung cancer (SCLC) (31). LCNEC and SCLC have been shown to be strongly related to smoking history, whereas TC and AC showed no association with smoking history (26, 27). Interestingly, evidence suggests that the 5-year survival rates of women and men with lung NETs are quite different. The prognosis of women with lung NETs was far better than that of men (32), suggesting that sex steroids and/or their receptors contribute significantly to the development and progression of lung NETs. How the expression of steroid hormone receptors, such as the PR, affects lung NETs is unclear.

The PR exists as two isoforms in most tissues, PRA and PRB. PRA lacks the first 164 amino acids at the N-terminus of PRB (33). Based on the phenotypes of the PR isoforms in selective knockout mice, PRB was shown to be more important for the proliferative responses to progesterone in the mammary epithelium, while ovarian and uterine development and function relied primarily on PRA (34). An increase in the relative levels of the PRA isoform over PRB is often found in a high fraction of atypical hyperplasia, ductal carcinoma in situ (DCIS), and invasive breast cancers (35, 36). The forced overexpression of a high PRA:PRB ratio in breast cancer cell lines led to an alteration of progestin-dependent effects on the cytoskeleton and cell motility (37). The overexpression of PRA or PRB in the mammary glands of transgenic mice results in abnormal mammary gland development (38). Thus, altered progesterone signaling through changes in the normal ratios of the two PR isoforms could significantly affect breast cancer progression (39).

In lung cancer, several lines of evidence suggested the significance of PR expression in non-small-cell lung cancer (NSCLC). Previous studies demonstrated that the expression of the PR in NSCLC is correlated with a less aggressive and more favorable prognosis (40-42), but another study failed to show such a correlation (43). Progesterone treatment of PR-positive NSCLC cells inhibited cell proliferation both *in vitro* and in a mouse xenograft model

(41, 42). Treatment with anti-progestin (Mifepristone or RU-486) reduced the progression of spontaneous lung tumors in mice (44). Lung tumors with little or no PR expression were shown to be highly aggressive (41) and to correlate with EGFR amplification (45). Our previous study demonstrated that PRB expression reduced EGF-induced NSCLC cell proliferation and the activation of ERK1/2 in the absence of progestin (46). While PR expression has previously been demonstrated in normal lung and lung NETs (47, 48), the role of the PR in the lung, especially in PNECs and lung NETs, remains unclear. As a first step towards understanding the role of the PR and PR isoforms in neuroendocrine cells of the lung, we examined the role of the PR and PR isoforms in PNECs of fetal and adult lung and determined how the differential expression of the PR isoforms affected lung NET cell proliferation.

Materials and Methods

Cell culture

HEK293T, T47D, and H727 cell lines were purchased from the American Type Culture Collection (ATCC). Cell line identities were confirmed by genomic DNA comparison to the ATCC database. HEK293T is a human embryonic kidney 293T cell line and was used for lentiviral production. T47D is a human breast ductal epithelial tumor cell line that expresses high levels of both PRA and PRB isoforms and was used as a positive control for PR expression. H727 is a PR-null bronchial carcinoid cell line that expresses p53 and EGF receptors and was used to construct a Tet-inducible PRA or PRB expression cell model. HEK293T and T47D cells were cultured in Dulbecco's Modified Eagle's Medium (DMEM; HyClone Laboratories, Logan, UT, USA) supplemented with 10% fetal bovine serum (FBS; Merck Millipore, Darmstadt, Germany) and 1% penicillin/streptomycin (Pen/Strep; HyClone Laboratories, Logan, UT, USA). H727 cells were maintained in Roswell Park Memorial Institute medium (RPMI; HyClone Laboratories, Logan, UT, USA) containing 10% FBS and 1% Pen/Strep. All cell lines were cultured in a 5% CO_2 humidified atmosphere at 37°C. All cell lines were routinely tested for mycoplasma contamination and were negative for mycoplasma contamination.

Real-time PCR

Real-time PCR was performed as previously described (46). Total RNA was extracted from T47D and H727 cell lines using GENEzol reagent (GeneAid, Taiwan). cDNA was generated from one microgram of total RNA using AccuPower RT Premix (Bioneer, Korea). cDNA was analyzed by real-time PCR with PR gene primers (forward primer: 5'TGGAAGAAATGACTGCATCG3', reverse primer: 5'TAGGGCTTGGCTTTCATTTG3') with a 195 bp PCR product (46) and GAPDH gene primers (forward primer: 5'ACATCGCTCAGACACCATG3', reverse primer: 5'TGTAGTTGAGGTCAATGAAGGG3') (49). PR and GAPDH amplifications were performed by using Green Star PCR Master Mix (Bioneer, Korea). The PCR gene product for the PR was analyzed by gel electrophoresis. T47D breast cancer cell cDNA was used as a positive control for PR expression. GAPDH served as an internal control. Samples without RNA templates were used as a negative control for genomic DNA contamination.

Lentiviral particle production

pHAGE-GFP, pHAGE-PRA, pHAGE-PRB, psPAX2, and pMD2 gene constructs were used to produce lentiviral particles by a method we previously described (46). cDNAs encoding PRA and PRB were amplified from pcDNAI-PRA and -PRB vectors, respectively (50). The pHAGE-Dest lentiviral vector, which is a Tet-On vector, encodes a recombinant tetracycline-controlled transcription factor (rtTA3) gene (51). Tet-inducible pHAGE-GFP, pHAGE-PRA or pHAGE-PRB lentiviral constructs in combination with psPAX2 (packaging plasmid) and pMD2.G (envelope plasmid) was used to construct lentiviral particles. psPAX2 contains genes that encode the following proteins and enzymes: Gag, Pro and Pol; pMD2.G encodes the gene VSV-G, which develops the lentiviral envelope; both plasmids were HIV-1-based.

To produce lentiviral particles carrying constructs for the Tet-inducible expression of GFP, PRA or PRB, HEK293T cells were seeded at 200,000 cells per well in 6-well tissue culture plates. After 24 hours, HEK293T cells reached 50–60% confluence and were treated with Opti-MEM I (Gibco/Life Technologies, Gaithersburg, MD, USA) mixed with packaging plasmid (psPAX2), envelope plasmid (pMD2.G), a DNA construct (pHAGE-GFP, pHAGE-PRA, pHAGE-PRB), and the X-tremeGENE HP DNA transfection reagent (Roche, Mannheim, Germany). psPAX2 and pMD2.G plasmids were provided by Didier Trono (Addgene plasmid #12260 and # 12259, respectively). The ratio of lentiviral DNA constructs with psPAX2:pMD2G was 1:2:2, and the ratio of DNA construct:XtremeGENE HP DNA transfection reagent was 1:3. Viral particle-containing media were collected 48 hours after transfection, filtered with 0.45 μM sterile filter PVDF membranes (Merck Millipore, Ireland), and stored at −80°C (52).

H727 cells expressing GFP or PRA or PRB by tetracycline-dependent construction

H727 cell models were constructed with modifications to a previously described method (46). Briefly, H727 cells were seeded at 500,000 cells per 100 x 20 mm tissue culture dish and incubated for 24 hours to achieve 50–60% confluence. Next, cells were treated with 2.5 ml of DMEM containing pHAGE-GFP, pHAGE-PRA or pHAGE-PRB viral particles mixed with 2.5 ml of serum-free RPMI medium and 8 μg/ml of polybrene transfection reagent (Merck Millipore, Darmstadt, Germany). Then, the cells in the virus-containing medium were incubated at 37°C for 4 hours, 5 ml of RPMI containing 10% FBS was added, and the cells were incubated overnight. The next day, the medium was changed to 10 ml of RPMI with 10% FBS, and the cells were incubated for an additional 48 hours. Transduced H727 cells were selected in RPMI medium with 10% FBS and 500 μg/ml of G418 (Gibco/Life Technologies, Gaithersburg, MD, USA) for 14 days. Doxycycline (Dox; Merck Millipore, Darmstadt, Germany) was added to induce GFP, PRA and PRB protein expression in the H727-GFP, H727-PRA and H727-PRB cell models (53). GFP expression in H727 cells was confirmed by GFP localization using fluorescence microscopy. H727-PRA and H727-PRB cell models have validated PRA or PRB protein expression, localization and transcriptional activity.

Western blot analysis

PRA and PRB protein expression were analyzed by western blot analysis as previously described (54). Briefly, cells were washed once with ice-cold phosphate buffered saline

(PBS; HyClone Laboratories, Logan, UT, USA). Cells were lysed with RIPA lysis buffer (Merck Millipore, Billerica, MA, USA), which contains a proteinase inhibitor cocktail (Roche, Mannheim, Germany), on ice for 5 min, scraped and collected. Equal amounts of protein in the cell lysate were separated by 10% sodium dodecyl sulfate-polyacrylamide gel electrophoresis (SDS-PAGE), and then, proteins were transferred to PVDF membranes. The membranes were incubated overnight at 4°C with a 1:2500 dilution of a primary antibody recognizing the PR (1294 PR, a specific mouse monoclonal antibody) (55), which detects PR isoforms A and B, or with a mouse monoclonal antibody IgG1 (250/H11 PR-B) that is specific for the PR-B isoform. The 250/H11 antibody was prepared against the purified amino-terminal domain of human PR (aa 1-535) as an antigen and was selected during a screening of hybridomas by high content immunofluorescence microscopy as previously described (56). As detected by western blotting in T47D whole cell lysate and immunofluorescence microscopy, the 250/H11 Mab has specificity for PR-B and fails to react with PR-A in different cell types engineered to express PR-A or PR-B separately. GAPDH antibody (Santa Cruz Biotechnology, CA, USA) at a 1:10000 (v/v) dilution was used as a loading control. Blots were washed with TBST buffer and incubated with the following secondary antibodies: anti-mouse IgG HRP-linked antibody (Cell Signaling Technology, Danvers, MA, USA) or anti-rabbit IgG HRP-linked antibody (Cell Signaling Technology, Danvers, MA, USA). Protein bands were detected on X-ray film by chemiluminescence reaction using Pierce® ECL Western Blotting Substrate (Thermo Scientific, Rockford, IL, USA).

Immunofluorescence

H727-PRA, H727-PRB and T47D cells (positive controls for PR expression (57, 58)) were seeded at 350,000 per well in 6-well tissue culture plates with coverslips in each well and were incubated at 37°C overnight to determine PRA and PRB protein localization. H727-GFP, H727-PRA, and H727-PRB cells were treated with 700 ng/ml of Dox for 24 hours to induce maximum GFP and PR expression. Then, H727-PRA and H727-PRB cells were treated with 10 nM progestin agonist R5020 (PerkinElmer, Boston, MA, USA) for 1 hour. Cells were then fixed in 4% paraformaldehyde for 20 min, washed with PBS three times, permeated with Triton X-100 for 10 min, washed with PBS three times and blocked with 1% FBS-PBS (Merck Millipore, Billerica, MA, USA) for 1 hour. Cells were incubated with a primary antibody against PR (1294 PR; mouse monoclonal antibody; 1:3000 dilution, 1% BSA-PBS (v/v)) or PRB (250H11 PRB-specific mouse monoclonal antibody; 1:1000 dilution, 1% BSA-PBS (v/v)) at 4°C overnight. Cells were washed and stained with secondary rabbit anti-mouse IgG-Alexa568 antibody at 1:5000 in 1% BSA-PBS (v/v) and counterstained with DAPI (4’,6-diamino-2-phenylindole) at 1:5000 in PBS (v/v) for 10 min. Cells were mounted onto slides with Prolong® Gold antifade reagent (Invitrogen, Carlsbad, CA, USA) and viewed on an LSM700 laser confocal scanning microscope (Carl Zeiss Microscopy GmbH, Oberkochen, Germany). Images were analyzed using ImageJ v 1.50 software (National Institute of Health, USA). The fluorescence intensities for each cell were obtained by selecting an area of interest of PR and PRB staining around the whole cell or nucleus, as previously described (46).

Immunocytochemistry of H727 cells

H727 cells were seeded 800,000 cells in a 10-cm tissue culture dish and incubated for 72 hours or approximately 80% confluency. Cells were transfected with 12.5 μg of pHAGE-GFP, pHAGE-PRA or pHAGE-PRB constructs. Twenty-four hours after transfection, cells were treated with 700 ng/ml of Dox for 24 hours to induce GFP or PR isoform expression. Cells were trypsinized, pelleted by centrifugation and fixed with 10% formalin for 10 min at room temperature. Large cell pellets were embedded in iPGell (Genostaff, Tokyo, Japan) and cut into thin paraffin sections. A Histofine Kit (Nichirei) was used for immunostaining as described by the manufacturer. PR (1294 PR; mouse monoclonal antibody; 1:1000 dilution) or PRB (250H11 PRB-specific mouse monoclonal antibody; 1:2000 dilution) were used to stain cell pellet sections. Cells were stained with a DAB (3,3′-diaminobenzidine tetrahydrochloride) solution to visualize the antigen-antibody complex in cells and counterstained with hematoxylin.

Luciferase assay

The transcriptional activities of PRA or PRB in H727, H727-PRA, and H727-PRB cells were examined. Cells were seeded at 100,000 cells per well in 24-well plates with RPMI supplemented with 5% DCC-FBS (Dextran-coated charcoal stripped FBS; Gibco/Life Technologies, Gaithersburg, MD, USA) and 1% Pen/Strep and were incubated overnight. Cells were transfected with 50 ng of pRL-CMV (Renilla) and 450 ng of PRE2-TK luciferase reporter constructs (54). Transient transfections were performed by using TurboFect™ Transfection Reagent (Thermo-Fisher Scientific, Waltham, MA, USA). After 24 hours, cells were treated with 700 ng/ml of Dox for 24 hours and then treated with 10 nM R5020 or ethanol (vehicle control) for an additional 24 hours. Next, cells were lysed with lysis buffer on ice, and cell lysates were collected and centrifuged at 8,000 x g for 10 min at 4°C. The luciferase activities of the cell lysates were analyzed using the Dual-Glo® Luciferase Assay System (Promega, Madison, WI USA) according to the manufacturer's recommendations.

Cell viability assay (MTT Assay)

Cell viability was examined using an MTT (3-(4,5-dimethylthiazol-2-yl)-2,5 diphenyltetrazolium bromide) assay. In MTT assays, cellular dehydrogenase enzymes in live cells react with the substrate (MTT) and produce a purple formazan dye. H727-GFP, H727-PRA, and H727-PRB were seeded at 15,000 cells per well in a 96-well tissue culture plate with RPMI medium supplemented with 5% DCC-FBS (Gibco/Life Technologies, Gaithersburg, MD, USA) and 1% Pen/Strep and incubated for 24 hours to achieve 50–60% confluence. Then, cells were treated with increasing concentrations of Dox (0, 50, 200, 500, 700 and 1000 ng/ml) for 48 hours to determine the optimal concentration for maximum PRA and PRB effects. In subsequent experiments, the effects of PRA or PRB protein expression were determined at the following time points: 0, 24, 48 and 72 hours. H727-PRA and H727-PRB were grown for 24 hours and treated with Dox (700 ng/ml); then, percent cell viability was measured at 0, 24, 48 and 72 hours after Dox treatment. To determine the effects of progestin and anti-progestin, cells were pretreated with Dox for 24 hours, treated with 10 nM R5020, 100 nM RU486 or a combination of R5020 and RU486 (59) and then incubated and measured at 0, 24, 48, and 72 hours. After treatment, 10 μl of MTT reagent (5 mg/ml)

(AppliChem, Darmstadt, Germany) was added to each well and incubated for 3 hours. The insoluble formazan in each well was dissolved with 100 μl of 10% SDS overnight. Plate absorbances were measured at 570 nm using a microplate spectrophotometer (Biotek Synergy Mx microplate reader, Biotek, USA), and all experiments were carried out in triplicate. Data were calculated from three independent experiments as the means ± SEM. The results are presented as percent cell viability relative to the control value of each experiment.

Tissue collection

We obtained 9 normal fetal (14–18 weeks old) and 10 adult tissue sections from the bronchi area of the lungs. Fetal cases were one female, one male, and seven unidentified sex. Adult cases were five females and 5 males. Normal lung tissues were serially prepared to compare staining between synaptophysin (SYN) and a double immunohistochemistry of SYN with PR or PRB. The Ethics Committees of Tohoku University Graduate School of Medicine and all participating institutions approved the protocol, No. 2018-1-32, used in this study.

Immunohistochemistry

Immunohistochemistry was conducted as previously described (60). Briefly, specimens were formalin-fixed and paraffin-embedded. A streptavidin-biotin amplification method via a Histofine Kit (Nichirei) was used for SYN immunohistochemistry. Paraffin-embedded specimens were cut into 3-μm-thick sections, mounted onto APES-coated slides, deparaffinized in xylene and rehydrated in alcohol. Antigen retrieval was performed by treating specimens with citrate buffer (2 mM citric acid and 9 mM trisodium citrate dihydrate, pH 6.0) and autoclaving at 121°C for 5 min. After antigen retrieval, samples were incubated with a rabbit-blocking solution (Nichirei Bioscience, Tokyo, Japan) at room temperature for 30 min. The slides were incubated at 4°C overnight with primary antibodies recognizing synaptophysin (DAKO, Tokyo, Japan). Next, the slides were incubated in peroxidase-conjugated streptavidin (Nichirei Bioscience) for 30 min at room temperature. Antigen-antibody complexes were visualized with 3,3′-diaminobenzidine tetrahydrochloride solution (1 mM DAB, 50 mM Tris-HCl buffer, pH 7.6, and 0.006% H_2O_2) and then counterstained with hematoxylin. Negative controls were obtained by incubation with rabbit immunoglobulin (DakoCytomation, Glostrup, Denmark; ref. No. X0936).

Double immunohistochemistry

Double immunohistochemistry staining was conducted as previously described (60). Fetal and adult normal lungs were fixed in 10% formalin and embedded in paraffin wax. Paraffin-embedded specimens were cut, mounted onto APES-coated slides, deparaffinized in xylene and rehydrated in alcohol. Antigen retrieval was performed by treating specimens with citrate buffer (2 mM citric acid and 9 mM trisodium citrate dihydrate, pH 6.0) and autoclaving at 121°C for 5 min. Then, samples were incubated with rabbit-blocking solution (Nichirei Bioscience, Tokyo, Japan) at room temperature for 30 min, incubated with primary antibody recognizing SYN (DAKO, Tokyo, Japan; 1:5000) or Ki-67 (DAKO, Tokyo, Japan; 1:100) at 4°C overnight and incubated with peroxidase-conjugated streptavidin (Nichirei Bioscience) for 30 min at room temperature. For the first antibody, antigen-antibody complexes were visualized with 1 mM DAB (50 mM Tris-HCl buffer, pH 7.6, and

0.006% H_2O_2). The same slides were subjected to antigen retrieval by treatment with citrate buffer (2 mM citric acid and 9 mM trisodium citrate dihydrate, pH 6.0), and then, samples were microwaved for 20 min. Samples were incubated with a rabbit-blocking solution at room temperature for 30 min. Then, samples were incubated at 4°C overnight with a primary antibody recognizing PR/PRB (1294 PR, a specific mouse monoclonal antibody) (55) or PRB (250H11 PRB-specific mouse monoclonal antibody). Next, the slides were incubated with biotin-labeled anti-mouse IgG and then with preformed avidin-biotin-alkaline phosphatase complexes. Vector Blue® (Vector Laboratories, Burlingame, CA) was used to visualize the PR (1294) or PRB (250H11) antibodies (blue) compared to SYN (brown).

Immunoreactivity scoring

Double immunohistochemistry staining of SYN^+PR^+, SYN^+PRB^+, $Ki\text{-}67^+PR^+$, and $Ki\text{-}67^+PRB^+$ was counted in each field and used to compare with SYN^+ immunohistochemistry by two observers (T. A and R.S). SYN^+ staining was used for comparison with the negative epithelial cells in the bronchi area. All normal lung staining was calculated as the ratio mean (60). Double immunohistochemistry and H-score analysis were defined by >2000 tumor cell counts.

Statistical analysis

Statistical analysis was conducted using JMP Pro software version 13.0.1 (SAS Institute, Cary, NC, USA) (61). Paired t-test or one-way ANOVA methods were used to evaluate associations among variables. Bonferroni's post hoc test correction was used when appropriate. Values were calculated from three independent experiments as the means ± SEM. Statistical significance was defined as p-values < 0.05 using a two-sided test.

Results

Characterization of Dox-inducible PRA and PRB expressing lung NET cell models

In a previous study, we demonstrated that PRB expression in NSCLC inhibits cell proliferation by interfering with the epidermal growth factor signaling (46). Whether the expression of the PR or PR isoform affects the growth of lung neuroendocrine cells is not known. Currently, there is no normal lung neuroendocrine cell line available for an *in vitro* study. In this study, we chose a bronchial carcinoid cell line (H727) as an *in vitro* model to examine the role of the PR and PR isoforms in normal/carcinoid lung neuroendocrine cells. H727 cells are well-differentiated bronchial carcinoid cells that express the NMB peptide and have p53 levels comparable to those found in the normal lung and demonstrate several aspects of normal neuroendocrine cells. Using RT-PCR and western blotting analyses, we showed that H727 cells did not express either isoform of the PR (PRA and/or PRB), and we could not detect any PR mRNA or protein in the H727 lung NET cells (Fig 1A-1C). These data demonstrated that H727 does not express endogenous PRs, allowing us to examine the role of these PR isoforms without interference from endogenous PRs by ectopically expressing inducible PRA or PRB in the H727 cells.

To examine how the expression of PRA or PRB affected the biological properties of H727, we constructed Dox-inducible PRA and PRB expression plasmids and introduced these constructs into H727 lung NET cells. Dox-inducible PRA or PRB (H727-PRA and H727-PRB) H727 cell models were constructed by transducing H727 cells with lentiviral constructs expressing Tet-inducible PRA or PRB, as described in the Materials and Methods section. Currently, most antibodies against the PR detect both PR isoforms, making it difficult to associate clinical outcomes with specific PR isoform expression in patient samples. To examine the role of PRB and PRA in lung neuroendocrine cells and in clinical specimens, we generated a new PRB-specific mouse monoclonal antibody (250H11 mAb) using a PRB-specific peptide as an immunogen, as described in the Materials and Methods section. As shown in Fig 2A by western blot analysis, the 250H11 mAb detected only PRB, while the 1294 mAb detected both the PRA and PRB isoforms in the H727-PRA and H727-PRB cells, respectively. Using immunofluorescence staining, we found that the PRB-specific antibody (250H11 mAb) stained the PR only in H727-PRB cells and not in H727-PRA cells (Fig 2B, panels D-F and J-L), while the 1294 mAb stained both PR isoforms (PRA and PRB) in the H727-PRA and H727-PRB cells (Fig 2B, panels A-C and G-I). We further examined the specificity of PR-250H11 by immunocytochemistry staining of H727-expressing GFP, PRA, or PRB cell paraffined sections with PR-250H11. As shown in Fig 2C, the PR-250H11 antibody stained only the cells expressing PRB with no cross-reactivity with cells expressing PR-An or GFP, while the PR antibody (1294 mAb) detected H727 cells expressing both isoforms of the PR (PRA and PRB) with no reactivity with cells expressing GFP (Fig 2C). Together, these data demonstrated the specificity of the 250H11 mAb in detecting the PRB isoform in cells by western blot and immunostaining.

We next examined the expression of Tet-inducible PR in the H727 cell model by western blot analyses. H727-PRA and H727-PRB cells were treated with increasing concentrations of a tetracycline analog (Doxycycline, Dox) at various time points (0, 24, 48, 72 and 96 hours). Cell lysates were analyzed for PR expression using a PR(PRA and PRB)-specific antibody, 1294 mAb. As shown in Fig 3A, the maximum PRA and PRB expression levels were observed when cells were treated with 700 ng/ml of Dox for 24 hours (Fig 3A).

To determine whether the Tet-inducible PRA and PRB properly localized inside the cells, we examined the intracellular localization of ectopic PRA and PRB in H727 cells. H727-PRA and H727-PRB cells were treated with 700 ng of Dox for 24 hours before treatment with R5020 for 60 mins. Cells were fixed, stained with PR (1294 mAb) and PRB (PRB-specific; 250H11 mAb) and analyzed by immunofluorescence. No PR staining was observed in the H727-PRA or PRB cells in the absence of Dox. Dox treatment induced PRA and PRB expression. PRA localized mainly in the nucleus, and progestin (R5020) treatment increased PRA nuclear localization, as detected by PR-specific 1294 mAb (Fig 2B, panels A-C); no PRA was detected by the PRB-specific 250H11 mAb (Fig 2B, panels D-F). PRB was distributed evenly between the nucleus and cytoplasm, and R5020 treatment promoted PRB nuclear localization, as detected by both the PR-specific 1294 mAb (Fig 2B, panels G-I) and PRB-specific 250H11 mAb (Fig 2B, panels J-L). Both H727-PRA and H727-PRB cells showed normal PR localization and proper nuclear translocation in response to the R5020 treatment, which was similar to the endogenous PR in T47D breast cancer cells (Fig 2B,

panels M-O). These data indicated that the expression and localization of the PR in H727 cells were similar to those of endogenous PR in T47D breast cancer cells.

To test whether the inducible PRA and PRB expressed in H727 cells were functional and transcriptionally active, H727-PRA and H727-PRB cells were transiently transfected with a PRE-luciferase reporter construct. Cells were then treated with 700 ng/ml of Dox for 24 hours prior to treatment with 10 nM R5020 for an additional 24 hours. The R5020 treatment significantly increased PRE-dependent luciferase activities over 10-fold in H727-PRB and only two-fold in H727-PRA (Fig 3B). Together, our data demonstrated that the PR isoforms expressed in H727 lung NETs were functional and had transcriptional activities similar to those expressed in breast cancer cells (62), with stronger PRB and weaker PRA transcriptional activities.

PRB and PRA expression inhibits H727 cell proliferation

It is unclear whether PR expression plays a role in lung neuroendocrine cell proliferation. Therefore, we examined the role of PRA and PRB expression on H727 cell proliferation. H727-GFP, H727-PRA, and H727-PRB cells were treated with increasing Dox concentrations (0, 50, 200, 500, 700 and 1000 ng/ml) for 24 hours. Cell proliferation was determined using an MTT assay as previously described (46). Dox treatment dose-dependently inhibited H727-PRA and H727-PRB cell proliferation with little to no effect on H727-GFP cells. The largest inhibition of cell proliferation was observed in H727-PRB cells treated with 700 ng/ml of Dox compared to H727-PRA and H727-GFP cells treated with a similar dose of Dox (Fig 4A). To determine the optimal time that PR isoform expression affected cell proliferation, H727-PRA and H727-PRB cells were treated with Dox 700 ng/ml for 24, 48 and 72 hours, and cell proliferation was determined by MTT assays at each time point (46). Dox-induced expression of PRA and PRB significantly decreased cell proliferation at all time points. The expression of PRB inhibited H727 cell proliferation more significantly than the expression of PRA at all time points tested (Fig 4B & 4C). The extent of PRB- and PRA-mediated inhibition of cell proliferation was comparable at all time points tested. The maximum percent inhibition of cell proliferation in H727 cells expressing PRB and PRA compared to parental H727 cells was 30.1 ± 3.1% and 19.2 ± 3.3%, respectively, and was observed at 48 hours after Dox induction (Fig 4B & 4C). Interestingly, the PR agonist (R5020) and antagonist (RU486) treatment of H727-PRA and H727-PRB had little to no effect on the inhibition of H727 cell proliferation. Together, these data suggested that the expression of PRA and PRB inhibited H727 lung NET cell proliferation and that the majority of the PR-mediated inhibition was dependent on receptor expression but independent of the PR ligand (Fig 4D and 4E).

PR expression in the pulmonary neuroendocrine cells (PNECs) of normal fetal and adult lung

While PR expression has been documented in the lung, the role of the PR in the neuroendocrine cells of the lung remains unclear. As a first step towards a better understanding of the role of the PR in lung neuroendocrine cells, we examined how the expression of the PR or PRB isoform in normal fetal and adult lung affected PNEC

proliferation during development. Fetal and adult lung tissues were collected and cut into three serial sections. The middle (second) section was single-stained with a monoclonal antibody against synaptophysin (SYN) to locate the neuroendocrine cells in lung tissues (Fig 5A & 5D). The top (first) and bottom (third) sections were double-stained with SYN and PR (1294) or PRB (250H11) mAb, respectively (Fig 5B-5C and 5E-5F). The number of SYN-positive cells in normal fetal lung was significantly higher than that in normal adult lung (Fig 5A and 5D). Double staining of SYN & PR and SYN & PRB demonstrated that a subset of SYN-positive PNECs expressed the PR and PRB. The PR (PRA and PRB) was significantly expressed more than PRB alone in PNECs in both the fetal and adult lung (Table 1). Among SYN-positive PNECs, there was a significantly higher percentage of cells that stained positive for PR (75.86±17.21%) and PRB (56.05±19.78%) in the fetal lung compared to the percentage of cells that stained positive for PR (56.62±26.12%) and PRB (32.54±18.31%) in the adult lung (Fig 5B, 5C, 5E and 5F) (Table 1 and 2). To our knowledge, this is the first report demonstrating PR and PRB expression in the PNECs of normal fetal and adult lungs. Further studies are needed to determine the biological role of the PR and progesterone in PNECs and in lung development.

PRB expression is associated with lower cell proliferation in fetal and adult lung PNECs.—Since the PR was found to be expressed in fetal and adult lung PNECs, we next examined how PR or PRB expression affected PNEC proliferation using immunohistochemistry of serial sections from fetal and adult lung tissues. Fetal and adult lung tissues were serially cut into three sections. The middle section was single-stained with a monoclonal antibody against SYN to locate the SYN-positive PNECs in lung tissue (Fig 6A & 6B). The top and bottom sections were double-stained with Ki-67 & PR (1294 mAb) or Ki-67 & PRB (250H11 mA), respectively (Fig 6B-6C and 6E-6F). As shown in Fig 5, fetal lung PNECs showed a higher percentage of cells stained positive for PR and PRB compared to adult PNECs. (Fig 5A-5F) (Table 2). However, both PR and PRB expression among the SYN-positive PNECs in the adult lung were significantly associated with cell proliferation, with significantly higher numbers of Ki-67-positive cells than those found in the fetal lung. The percentages of cells stained positive for both PR and Ki-67 were 91.53±7.34% and 57.64±7.71% in the adult and fetal lung, respectively. The percentages of cells stained positive for both PRB and Ki-67 were 57.37±13.02% and 41.27±7.91% in the adult and fetal lung, respectively (Fig 6B, 6C, 6E, and 6F) (Table 2). Together, our data suggests that PR expression was significantly associated with a higher cell proliferation than PRB expression in SYN-positive PNECs in both the fetal and adult lung (Table 1). Interestingly, the expression of PRB affected cell proliferation more than the expression of PR in the adult lung compared to the fetal lung. As shown in Table 1, the percentage of positive cell differences between PR+:Ki-67 and PRB+:Ki67 was 34.16±18.17% in the adult lung and 16.37±10.78 in the fetal lung. Together, our data suggests that the expression of the PR isoforms could significantly affect PNEC proliferation, especially in the adult lung.

Discussion

The PR is expressed in several tissues in the body, including both reproductive and nonreproductive tissues (63-67) . While the roles of the PR and PR isoforms have been

well studied in reproductive tissues, their roles in nonreproductive tissues are not well understood. We and others have shown that PRB expression in NSCLC is correlated with lower cell proliferation and associated with a better prognosis (46). However, whether the PR is expressed and how PR and PR isoform expression affect PNECs is largely unexplored. To better understand the role of PR and PR isoform expression in PNECs *in vitro*, H727, a well-differentiated bronchial carcinoid cell line with several features similar to PNECs in the lung, was used as a model. Using a Tet-inducible PR expression system, we demonstrated that PRA and PRB in the H727 cell line showed normal receptor localization and were transcriptionally active, similar to those found in breast cancer cells (68). In the absence of progesterone, PRB was evenly distributed in both the nucleus and cytoplasm, while PRA localized mainly in the nucleus with very limited cytoplasmic localization. Both PRA and PRB translocated to the nucleus upon addition of progestin. We further showed that both PRA and PRB were transcriptionally active and capable of trans-activating PRE-dependent gene expression (Fig 3B) in H727 cells. PRB was transcriptionally more active than PRA in H727, similar to PRs expressed in breast cancer cells (Fig 3B) (33, 69).

We used the Tet-inducible expression of GFP, PRA or PRB in H727 cell models so that we could directly determine and compare the role of PR and PR isoform expression on PNEC proliferation. The expression of both PR isoforms inhibited H727 cell proliferation, while the expression of the unrelated protein, GFP, had no effect on H727 cell proliferation (Fig 4A). Furthermore, the expression of PRB significantly inhibited H727 cell proliferation better than that of PRA (Fig 4A-4C). Interestingly, the addition of PR ligands, either agonist R5020 or antagonist RU486, had no significant effects on the cell expressing both PR isoforms, suggesting that the PR-mediated inhibition of H727 was dependent on the expression of the PR but independent of the expression of its ligand.

The PR has been shown to function in a ligand-independent manner. Most studies to date have shown PR-stimulated transcription or cell proliferation in the absence of PR ligands in breast cancer cell models. Several studies demonstrated a ligand-independent PR activation in breast cancer cells (70). The phosphorylation of Ser400 in the PR by CDK2 was shown to induce PR nuclear localization and transcriptional activity (71). PR phosphorylation and sumoylation were shown to induce PR transcription, independent of ligand, and promote breast cancer cell proliferation (72). We previously demonstrated that PRB expression, independent of ligand, inhibited cell proliferation and blunted EGFR-mediated signaling in the A549 NSCLC cell model (46). We further showed that the expression of PRB with a mutation in the polyproline domain (PPD), a ligand for SH3 domains, (PRBΔSH3) abolished the ability of PRB to inhibit NSCLC cell proliferation and interfere with EGFR signaling. Thus, PR extranuclear signaling through PPD-SH3 interactions may contribute significantly to the PR-mediated inhibition of H727 cell proliferation by interfering with growth factor signaling, as shown in the NSCLC cell model (46).

Our results were based on a PR-specific 1294 antibody (55) that detected both PR isoforms (PRA and PRB), and the new PRB-specific 250H11 antibody, which was highly specific for detecting PRB but not PRA. Antibody specificities were confirmed by western blot, immunofluorescence and immunocytochemistry analyses in T47D breast cancer cells and H727 cell lines expressing either PRA or PRB (Fig 3A and 3B). Unlike the previously

described PR isoform-specific antibodies (73-75), the 250H11 antibody does not require any blocking peptides to confer PRB specificity, making it easy to use in routine immunohistochemical examination to explore the role of the PRB isoform.

Several studies have reported that lung NETs arise from PNECs, which are often found in the bronchiolar epithelium of the lung (25, 76). In fetuses, PNECs are crucial for lung development. PNECs secrete amines and peptides such as synaptophysin or chromogranin A (19). It is unclear whether sex steroid hormones and their receptors, such as the PR, play a role in lung development. While PR expression has been documented in the lung (77), its role in lung development remains poorly understood. In this study, we showed the expression of PR (PRA and PRB) and PRB isoforms in normal fetal and adult lungs and in PNECs. To our knowledge, this is the first report demonstrating PR expression in the PNECs of normal fetal and adult lungs. PR expression in PNECs was higher in the fetal lung than in the adult lung. Interestingly, PRB expression was higher in the fetal lung than in the adult lung, suggesting that expression of PRB in the developing fetal lung could play a role during lung development. Moreover, our data demonstrated that PRs or PRB are often found in SYN-positive PNECs. PNECs have been shown to be involved in the development of the breathing control system (78, 79), suggesting that PRs or PRB could play a role in the development and function of the lung breathing control system. In addition to localizing PRs and PRB in PNECs, we also found that PRB expression was associated with a significantly lower percentage of Ki-67-positive proliferating cells compared to PR expression in PNECs. However, the expression of the PR and PRB in the adult lung was associated with a higher percentage of Ki-67-positive proliferating cells compared to the expression of the PR and PRB in the fetal lung. Together, our data suggests that the expression of the PR and PRB in PNECs affected cell proliferation in the fetal lung more than in the adult lung. A recent attempt to generate a normal neuroendocrine cell line failed to obtain a continuous culture *in vitro* (80). No normal neuroendocrine cell line is currently available. In this study, we used H727 neuroendocrine carcinoid cells as a model for normal/carcinoid PNECs. The H727 cell line was chosen for this study because it was demonstrated in several studies to be superior compared to the other available bronchial carcinoid lines, with detectable levels of p53 mRNA, which are comparable to those found in normal lung (70)(81, 82). However, it is important to note that recent next generation exome-level sequencing data suggested that mutations and copy number variations in frequently used pulmonary neuroendocrine carcinoid cell lines, including H727, were more similar to those of primary high-grade small-cell lung cancer than those of primary pulmonary carcinoids (83). Thus, it is arguable whether the results obtained from the H727 cell model could be replicated in normal PNECs. Interestingly, we found that PRB expression in both normal fetal and adult PNECs is associated with low cell proliferation, similar to results observed in the H727 cell model, suggesting that mutations found in H727 might not significantly affect PR signaling and that the results obtained from the H727 cell model were physiologically relevant. Nevertheless, it will be interesting to evaluate and confirm the effects of the PR isoforms in primary organoid cultures of pulmonary PNECs in the future.

The PR has been routinely used as a marker to help classify breast cancer patients for targeted treatment. Currently, little is known about the role of the PR or progesterone in lung diseases, especially in neuroendocrine tumors (NETs). Based on our results in this study,

PRB expression is associated with low cell proliferation and may be used as a prognostic marker for lung NETs. Additionally, our results may serve as a basis for the development of a novel class of drugs for lung NET treatment by enhancing PRB expression. Nevertheless, future studies on progesterone, PR and PR isoform expression in association with patients' clinical outcomes are needed to carefully examine a potential role for using the PR as a marker to help improve lung NET treatment in the future.

In conclusion, we demonstrated that PNECs expressing PRB are associated with a lower cell proliferation than PNECs expressing the PR (both PRA and PRB), both *in vitro* and in clinical samples. A better understanding of the molecular mechanisms involved in PR and PR isoform signaling in PNECs and lung NET cells may help in developing novel therapeutic strategies to treat lung diseases and benefit lung NET patients in the future.

Acknowledgments

This work was supported by a grant from the Chulalongkorn University's 90th Anniversary Fund (Ratchadaphisek Somphot Endowment Fund Grant) to T.A. and a grant from Chulalongkorn University (GB-A_60_037_37_02) to V.B. PR monoclonal antibody production was performed by the Protein and Monoclonal Antibody Production Core facility at the Baylor College of Medicine Dan L. Duncan Comprehensive Cancer Center (Houston, Texas, USA) and was supported by an NCI Cancer Center Support Grant (P30CA125123) to D.P.E. We thank Kurt Christensen and Karen Moberg in the BCM Core for PR antibody production and Celetta Callaway for antibody purification.

References

1. Trotter A, Ebsen M, Kiossis E, Meggle S, Kueppers E, Beyer C, et al. Prenatal estrogen and progesterone deprivation impairs alveolar formation and fluid clearance in newborn piglets. Pediatric research. 2006;60(1):60–4. [PubMed: 16690946]
2. Sweezey N, Tchepichev S, Gagnon S, Fertuck K, O'Brodovich H. Female gender hormones regulate mRNA levels and function of the rat lung epithelial Na channel. The American journal of physiology. 1998;274(2 Pt 1):C379–86. [PubMed: 9486127]
3. Trotter A, Kipp M, Schrader RM, Beyer C. Combined application of 17beta-estradiol and progesterone enhance vascular endothelial growth factor and surfactant protein expression in cultured embryonic lung cells of mice. International journal of pediatrics. 2009;2009:170491. [PubMed: 19946415]
4. Nielsen HC, Torday JS. Sex differences in fetal rabbit pulmonary surfactant production. Pediatric research. 1981;15(9):1245–7. [PubMed: 6895251]
5. Bayliss DA, Millhorn DE, Gallman EA, Cidlowski JA. Progesterone stimulates respiration through a central nervous system steroid receptor-mediated mechanism in cat. Proceedings of the National Academy of Sciences of the United States of America. 1987;84(21):7788–92. [PubMed: 3478727]
6. Tatsumi K, Mikami M, Kuriyama T, Fukuda Y. Respiratory stimulation by female hormones in awake male rats. Journal of applied physiology (Bethesda, Md : 1985). 1991;71(1):37–42. [PubMed: 1717425]
7. Verma MK, Miki Y, Sasano H. Sex steroid receptors in human lung diseases. J Steroid Biochem Mol Biol. 2011;127:216–22. [PubMed: 21856418]
8. Beyer C, Kuppers E, Karolczak M, Trotter A. Ontogenetic expression of estrogen and progesterone receptors in the mouse lung. Biology of the neonate. 2003;84(1):59–63. [PubMed: 12890938]
9. Massaro D, Clerch LB, Massaro GD. Estrogen receptor-α regulates pulmonary alveolar loss and regeneration in female mice: morphometric and gene expression studies. American Journal of Physiology-Lung Cellular and Molecular Physiology. 2007;293(1):L222–L8. [PubMed: 17449797]
10. Hanley K, Rassner U, Jiang Y, Vansomphone D, Crumrine D, Komüves L, et al. Hormonal basis for the gender difference in epidermal barrier formation in the fetal rat. Acceleration by estrogen and delay by testosterone. The Journal of clinical investigation. 1996;97(11):2576–84. [PubMed: 8647951]

11. Marquez-Garban DC, Mah V, Alavi M, Maresh EL, Chen H-W, Bagryanova L, et al. Progesterone and estrogen receptor expression and activity in human non-small cell lung cancer. Steroids. 2011;76(9):910–20. [PubMed: 21600232]
12. Zarazúa A, González-Arenas A, Ramírez-Vélez G, Bazán-Perkins B, Guerra-Araiza C, Campos-Lara MG. Sexual Dimorphism in the Regulation of Estrogen, Progesterone, and Androgen Receptors by Sex Steroids in the Rat Airway Smooth Muscle Cells. International Journal of Endocrinology. 2016;2016:8423192. [PubMed: 27110242]
13. Popovic RM, White DP. Upper airway muscle activity in normal women: influence of hormonal status. Journal of applied physiology (Bethesda, Md : 1985). 1998;84(3):1055–62. [PubMed: 9480969]
14. Cutz E Neuroendocrine cells of the lung an overview of morphologic characteristics and development. Experimental lung research. 1982;3(3-4):185–208.
15. Boers JE, den Brok JL, Koudstaal J, Arends JW, Thunnissen FB. Number and proliferation of neuroendocrine cells in normal human airway epithelium. American journal of respiratory and critical care medicine. 1996;154(3 Pt 1):758–63. [PubMed: 8810616]
16. Cutz E, Perrin DG, Pan J, Haas EA, Krous HF. Pulmonary neuroendocrine cells and neuroepithelial bodies in sudden infant death syndrome: potential markers of airway chemoreceptor dysfunction. Pediatric and developmental pathology : the official journal of the Society for Pediatric Pathology and the Paediatric Pathology Society. 2007;10(2):106–16. [PubMed: 17378691]
17. Cutz E, Yeger H, Pan J. Pulmonary neuroendocrine cell system in pediatric lung disease-recent advances. Pediatric and developmental pathology : the official journal of the Society for Pediatric Pathology and the Paediatric Pathology Society. 2007;10(6):419–35. [PubMed: 18001162]
18. Gosney JR. Neuroendocrine cell populations in postnatal human lungs: minimal variation from childhood to old age. The Anatomical record. 1993;236(1):177–80. [PubMed: 8507004]
19. Van Lommel A, Bolle T, Fannes W, Lauweryns JM. The pulmonary neuroendocrine system: the past decade. Archives of histology and cytology. 1999;62(1):1–16. [PubMed: 10223738]
20. Cutz E, Speirs V, Yeger H, Newman C, Wang D, Perrin DG. Cell biology of pulmonary neuroepithelial bodies--validation of an in vitro model. I. Effects of hypoxia and Ca2+ ionophore on serotonin content and exocytosis of dense core vesicles. The Anatomical record. 1993;236(1):41–52. [PubMed: 8507015]
21. King KA, Torday JS, Sunday ME. Bombesin and [Leu8]phyllolitorin promote fetal mouse lung branching morphogenesis via a receptor-mediated mechanism. Proceedings of the National Academy of Sciences of the United States of America. 1995;92(10):4357–61. [PubMed: 7753811]
22. Sunday ME, Hua J, Torday JS, Reyes B, Shipp MA. CD10/neutral endopeptidase 24.11 in developing human fetal lung. Patterns of expression and modulation of peptide-mediated proliferation. Journal of Clinical Investigation. 1992;90(6):2517–25. [PubMed: 1469102]
23. King KA, Hua J, Torday JS, Drazen JM, Graham SA, Shipp MA, et al. CD10/neutral endopeptidase 24.11 regulates fetal lung growth and maturation in utero by potentiating endogenous bombesin-like peptides. Journal of Clinical Investigation. 1993;91(5):1969–73. [PubMed: 8486767]
24. Ito T, Udaka N, Yazawa T, Okudela K, Hayashi H, Sudo T, et al. Basic helix-loop-helix transcription factors regulate the neuroendocrine differentiation of fetal mouse pulmonary epithelium. Development (Cambridge, England). 2000;127(18):3913–21. [PubMed: 10952889]
25. Yao JC, Hassan M, Phan A, Dagohoy C, Leary C, Mares JE, et al. One Hundred Years After “Carcinoid”: Epidemiology of and Prognostic Factors for Neuroendocrine Tumors in 35,825 Cases in the United States. Journal of Clinical Oncology. 2008;26(18):3063–72. [PubMed: 18565894]
26. Gustafsson BI, Kidd M, Chan A, Malfertheiner MV, Modlin IM. Bronchopulmonary neuroendocrine tumors. Cancer. 2008;113(1):5–21. [PubMed: 18473355]
27. Rekhtman N Neuroendocrine tumors of the lung: an update. Archives of pathology & laboratory medicine. 2010;134(11):1628–38. [PubMed: 21043816]
28. Caplin ME, Baudin E, Ferolla P, Filosso P, Garcia-Yuste M, Lim E, et al. Pulmonary neuroendocrine (carcinoid) tumors: European Neuroendocrine Tumor Society expert consensus and recommendations for best practice for typical and atypical pulmonary carcinoids. Annals of

oncology : official journal of the European Society for Medical Oncology. 2015;26(8):1604–20. [PubMed: 25646366]

29. Bertino EM, Confer PD, Colonna JE, Ross P, Otterson GA. Pulmonary neuroendocrine/carcinoid tumors: a review article. Cancer. 2009;115(19):4434–41. [PubMed: 19562772]
30. Kulke MH, Mayer RJ. Carcinoid tumors. The New England journal of medicine. 1999;340(11):858–68. [PubMed: 10080850]
31. Hendifar AE, Marchevsky AM, Tuli R. Neuroendocrine Tumors of the Lung: Current Challenges and Advances in the Diagnosis and Management of Well-Differentiated Disease. Journal of thoracic oncology : official publication of the International Association for the Study of Lung Cancer. 2017;12(3):425–36. [PubMed: 27890494]
32. Tsai H-J, Wu C-C, Tsai C-R, Lin S-F, Chen L-T, Chang JS. The Epidemiology of Neuroendocrine Tumors in Taiwan: A Nation-Wide Cancer Registry-Based Study. PLoS ONE. 2013;8(4):e62487. [PubMed: 23614051]
33. Kastner P, Krust A, Turcotte B, Stropp U, Tora L, Gronemeyer H, et al. Two distinct estrogen-regulated promoters generate transcripts encoding the two functionally different human progesterone receptor forms A and B. EMBO J. 1990;9(5):1603–14. [PubMed: 2328727]
34. Giangrande PH, Kimbrel EA, Edwards DP, McDonnell DP. The opposing transcriptional activities of the two isoforms of the human progesterone receptor are due to differential cofactor binding. Molecular and Cellular Biology. 2000;20(9):3102–15. [PubMed: 10757795]
35. Hopp TA, Weiss HL, Hilsenbeck SG, Cui Y, Allred DC, Horwitz KB, et al. Breast cancer patients with progesterone receptor PR-A-rich tumors have poorer disease-free survival rates. Clin Cancer Res. 2004;10(8):2751–60. [PubMed: 15102680]
36. Mote PA, Bartow S, Tran N, Clarke CL. Loss of co-ordinate expression of progesterone receptors A and B is an early event in breast carcinogenesis. Breast Cancer Res Treat. 2002;72(2):163–72. [PubMed: 12038707]
37. McGowan EJ, Clark CL. Effect of over-expression of progesterone receptor A on endogenous progestin-sensitive endpoints in breast cancer cells. Mol Endocrinol. 1999;13:1657–71. [PubMed: 10517668]
38. Shyamala G, Yang X, Silberstein G, Barcellos-Hoff MH, Dale E. Transgenic mice carrying an imbalance in the native ratio of A to B forms of progesterone receptor exhibit developmental abnormalities in mammary glands. Proc Natl Acad Sci U S A. 1998;95(2):696–701. [PubMed: 9435255]
39. Graham JD, Yager ML, Hill HD, Byth K, O'Neill GM, Clarke CL. Altered progesterone receptor isoform expression remodels progestin responsiveness of breast cancer cells. Mol Endocrinol. 2005;19(11):2713–35. [PubMed: 15976005]
40. Raso MG, Behrens C, Herynk MH, Liu S, Prudkin L, Ozburn NC, et al. Immunohistochemical expression of estrogen and progesterone receptors identifies a subset of NSCLCs and correlates with EGFR mutation. Clin Cancer Res. 2009;15(17):5359–68. [PubMed: 19706809]
41. Ishibashi H, Suzuki T, Suzuki S, Niikawa H, Lu L, Miki Y, et al. Progesterone receptor in non-small cell lung cancer--a potent prognostic factor and possible target for endocrine therapy. Cancer Res. 2005;65(14):6450–8. [PubMed: 16024650]
42. Marquez-Garban DC, Mah V, Alavi M, Maresh EL, Chen HW, Bagryanova L, et al. Progesterone and estrogen receptor expression and activity in human non-small cell lung cancer. Steroids. 2011;76(9):910–20. [PubMed: 21600232]
43. Sun S, Schiller JH, Gazdar AF. Lung cancer in never smokers--a different disease. Nature reviews. 2007;7(10):778–90.
44. Check JH, Sansoucie L, Chern J, Dix E. Mifepristone treatment improves length and quality of survival of mice with spontaneous lung cancer. Anticancer research. 2010;30(1):119–22. [PubMed: 20150625]
45. Sun HB, Zheng Y, Ou W, Fang Q, Li P, Ye X, et al. Association between hormone receptor expression and epidermal growth factor receptor mutation in patients operated on for non-small cell lung cancer. Ann Thorac Surg. 2011;91(5):1562–7. [PubMed: 21524465]
46. Kawprasertsri S, Pietras RJ, Marquez-Garban DC, Boonyaratanakornkit V. Progesterone receptor (PR) polyproline domain (PPD) mediates inhibition of epidermal growth factor receptor (EGFR)

signaling in non-small cell lung cancer cells. Cancer letters. 2016;374(2):279–91. [PubMed: 26892043]

47. Curioni-Fontecedro A, Soldini D, Seifert B, Eichmueller T, Korol D, Moch H, et al. A comprehensive analysis of markers for neuroendocrine tumors of the lungs demonstrates estrogen receptor beta to be a prognostic markers in SCLC male patients. Journal of Cytology & Histology. 2014;5(5):1.
48. Sica G, Wagner PL, Altorki N, Port J, Lee PC, Vazquez MF, et al. Immunohistochemical expression of estrogen and progesterone receptors in primary pulmonary neuroendocrine tumors. Archives of pathology & laboratory medicine. 2008;132(12):1889–95. [PubMed: 19061285]
49. Udommethaporn S, Tencomnao T, McGowan EM, Boonyaratanakornkit V. Assessment of Anti-TNF-alpha Activities in Keratinocytes Expressing Inducible TNF- alpha: A Novel Tool for Anti-TNF-alpha Drug Screening. 2016;11(7):e0159151.
50. Boonyaratanakornkit V, Scott MP, Ribon V, Sherman L, Anderson SM, Maller JL, et al. Progesterone receptor contains a proline-rich motif that directly interacts with SH3 domains and activates c-Src family tyrosine kinases. Mol Cell. 2001;8(2):269–80. [PubMed: 11545730]
51. Meerbrey KL, Hu G, Kessler JD, Roarty K, Li MZ, Fang JE, et al. The pINDUCER lentiviral toolkit for inducible RNA interference in vitro and in vivo. Proceedings of the National Academy of Sciences of the United States of America. 2011;108(9):3665–70. [PubMed: 21307310]
52. Alexeyev MF, Fayzulin R, Shokolenko IN, Pastukh V. A retro-lentiviral system for doxycycline-inducible gene expression and gene knockdown in cells with limited proliferative capacity. Molecular biology reports. 2010;37(4):1987–91. [PubMed: 19655272]
53. Krishnapuram R, Dhurandhar EJ, Dubuisson O, Hegde V, Dhurandhar NV. Doxycycline-regulated 3T3-L1 preadipocyte cell line with inducible, stable expression of adenoviral E4orf1 gene: a cell model to study insulin-independent glucose disposal. PLoS One. 2013;8(3):e60651. [PubMed: 23544159]
54. Boonyaratanakornkit V, Melvin V, Prendergast P, Altmann M, Ronfani L, Bianchi ME, et al. High-mobility group chromatin proteins 1 and 2 functionally interact with steroid hormone receptors to enhance their DNA binding in vitro and transcriptional activity in mammalian cells. Mol Cell Biol. 1998;18(8):4471–87. [PubMed: 9671457]
55. Clemm DL, Sherman L, Boonyaratanakornkit V, Schrader WT, Weigel NL, Edwards DP. Differential hormone-dependent phosphorylation of progesterone receptor A and B forms revealed by a phosphoserine site-specific monoclonal antibody. Mol Endocrinol. 2000;14(1):52–65. [PubMed: 10628747]
56. Szafran AT, Mancini MG, Nickerson JA, Edwards DP, Mancini MA. Use of HCA in subproteome-immunization and screening of hybridoma supernatants to define distinct antibody binding patterns. Methods. 2016;96:75–84. [PubMed: 26521976]
57. Savouret JF, Fridlanski F, Atger M, Misrahi M, Berger R, Milgrom E. Origin of the high constitutive level of progesterone receptor in T47-D breast cancer cells. Molecular and cellular endocrinology. 1991;75(2):157–62. [PubMed: 2050275]
58. Vladusic EA, Hornby AE, Guerra-Vladusic FK, Lakins J, Lupu R. Expression and regulation of estrogen receptor beta in human breast tumors and cell lines. Oncology reports. 2000;7(1):157–67. [PubMed: 10601611]
59. McGowan EM, Russell AJ, Boonyaratanakornkit V, Saunders DN, Lehrbach GM, Sergio CM, et al. Progestins reinitiate cell cycle progression in antiestrogen-arrested breast cancer cells through the B-isoform of progesterone receptor. Cancer Res. 2007;67(18):8942–51. [PubMed: 17875737]
60. Yazdani S, Miki Y, Tamaki K, Ono K, Iwabuchi E, Abe K, et al. Proliferation and maturation of intratumoral blood vessels in non-small cell lung cancer. Human pathology. 2013;44(8):1586–96. [PubMed: 23522064]
61. Miyashita M, Sasano H, Tamaki K, Hirakawa H, Takahashi Y, Nakagawa S, et al. Prognostic significance of tumor-infiltrating CD8(+) and FOXP3(+) lymphocytes in residual tumors and alterations in these parameters after neoadjuvant chemotherapy in triple-negative breast cancer: a retrospective multicenter study. Breast Cancer Research : BCR. 2015;17(1):124. [PubMed: 26341640]

62. Giangrande PH, Kimbrel EA, Edwards DP, McDonnell DP. The opposing transcriptional activities of the two isoforms of the human progesterone receptor are due to differential cofactor binding. Mol Cell Biol. 2000;20(9):3102–15. [PubMed: 10757795]
63. Bland R Steroid hormone receptor expression and action in bone. Clinical science (London, England : 1979). 2000;98(2):217–40. [PubMed: 10657279]
64. Graham JD, Clarke CL. Physiological action of progesterone in target tissues. Endocrine reviews. 1997;18(4):502–19. [PubMed: 9267762]
65. Han Y, Feng HL, Sandlow JI, Haines CJ. Comparing expression of progesterone and estrogen receptors in testicular tissue from men with obstructive and nonobstructive azoospermia. Journal of andrology. 2009;30(2):127–33. [PubMed: 18835831]
66. Ozawa H Steroid Hormones, their receptors and neuroendocrine system. Journal of Nippon Medical School = Nippon Ika Daigaku zasshi. 2005;72(6):316–25. [PubMed: 16415511]
67. Tincello DG, Taylor AH, Spurling SM, Bell SC. Receptor isoforms that mediate estrogen and progestagen action in the female lower urinary tract. The Journal of urology. 2009;181(3):1474–82. [PubMed: 19157432]
68. Lim CS, Baumann CT, Htun H, Xian W, Irie M, Smith CL, et al. Differential localization and activity of the A- and B-forms of the human progesterone receptor using green fluorescent protein chimeras. Molecular endocrinology (Baltimore, Md). 1999;13(3):366–75. [PubMed: 10076994]
69. Giangrande PH, McDonnell DP. The A and B isoforms of the human progesterone receptor: two functionally different transcription factors encoded by a single gene. Recent progress in hormone research. 1999;54:291–313; discussion -4. [PubMed: 10548881]
70. Denner LA, Weigel NL, Maxwell BL, Schrader WT, O'Malley BW. Regulation of progesterone receptor-mediated transcription by phosphorylation. Science (New York, NY). 1990;250(4988):1740–3.
71. Pierson-Mullany LK, Lange CA. Phosphorylation of Progesterone Receptor Serine 400 Mediates Ligand-Independent Transcriptional Activity in Response to Activation of Cyclin-Dependent Protein Kinase 2. Molecular and Cellular Biology. 2004;24(24):10542–57. [PubMed: 15572662]
72. Daniel AR, Lange CA. Protein kinases mediate ligand-independent derepression of sumoylated progesterone receptors in breast cancer cells. Proceedings of the National Academy of Sciences of the United States of America. 2009;106(34):14287–92. [PubMed: 19706513]
73. Graham JD, Yeates C, Balleine RL, Harvey SS, Milliken JS, Bilous AM, et al. Characterization of progesterone receptor A and B expression in human breast cancer. Cancer Research. 1995;55(21):5063–8. [PubMed: 7585552]
74. Lorenzo F, Jolivet A, Loosfelt H, Thu vu Hai M, Brailly S, Perrot-Applanat M, et al. A rapid method of epitope mapping. Application to the study of immunogenic domains and to the characterization of various forms of rabbit progesterone receptor. European journal of biochemistry. 1988;176(1):53–60. [PubMed: 2458256]
75. Clarke CL, Zaino RJ, Feil PD, Miller JV, Steck ME, Ohlsson-Wilhelm BM, et al. Monoclonal antibodies to human progesterone receptor: characterization by biochemical and immunohistochemical techniques. Endocrinology. 1987;121(3):1123–32. [PubMed: 3304978]
76. Giangreco A, Reynolds SD, Stripp BR. Terminal Bronchioles Harbor a Unique Airway Stem Cell Population That Localizes to the Bronchoalveolar Duct Junction. The American Journal of Pathology. 2002;161(1):173–82. [PubMed: 12107102]
77. Press M, Spaulding B, Groshen S, Kaminsky D, Hagerty M, Sherman L, et al. Comparison of different antibodies for detection of progesterone receptor in breast cancer. Steroids. 2002;67(9):799–813. [PubMed: 12123792]
78. Sunday ME, Cutz E. Role of neuroendocrine cells in fetal and postnatal lung. Endocrinology of the Lung: Springer; 2000. p. 299–336.
79. Cutz E, Fu X, Yeger H, Peers C, Kemp P. Oxygen sensing in pulmonary neuroepithelial bodies and related tumor cell model. LUNG BIOLOGY IN HEALTH AND DISEASE. 2003;175:567–602.
80. Asiedu MK, Thomas CF Jr, Tomaszek SC, Peikert T, Sanyal B, Sutor SL, et al. Generation and sequencing of pulmonary carcinoid tumor cell lines. Journal of Thoracic Oncology. 2014;9(12):1763–71. [PubMed: 25226425]

81. Grozinsky-Glasberg S, Shimon I, Rubinfeld H. The role of cell lines in the study of neuroendocrine tumors. Neuroendocrinology. 2012;96(3):173–87. [PubMed: 22538498]

82. Hegedus TJ, Falzon M, Margaretten N, Gazdar AF, Schuller HM. Inhibition of N-diethylnitrosamine metabolism by human lung cancer cell lines with features of well differentiated pulmonary endocrine cells. Biochemical pharmacology. 1987;36(20):3339–43. [PubMed: 2823818]

83. Boora GK, Kanwar R, Kulkarni AA, Pleticha J, Ames M, Schroth G, et al. Exome-level comparison of primary well-differentiated neuroendocrine tumors and their cell lines. Cancer genetics. 2015;208(7):374–81. [PubMed: 26087898]

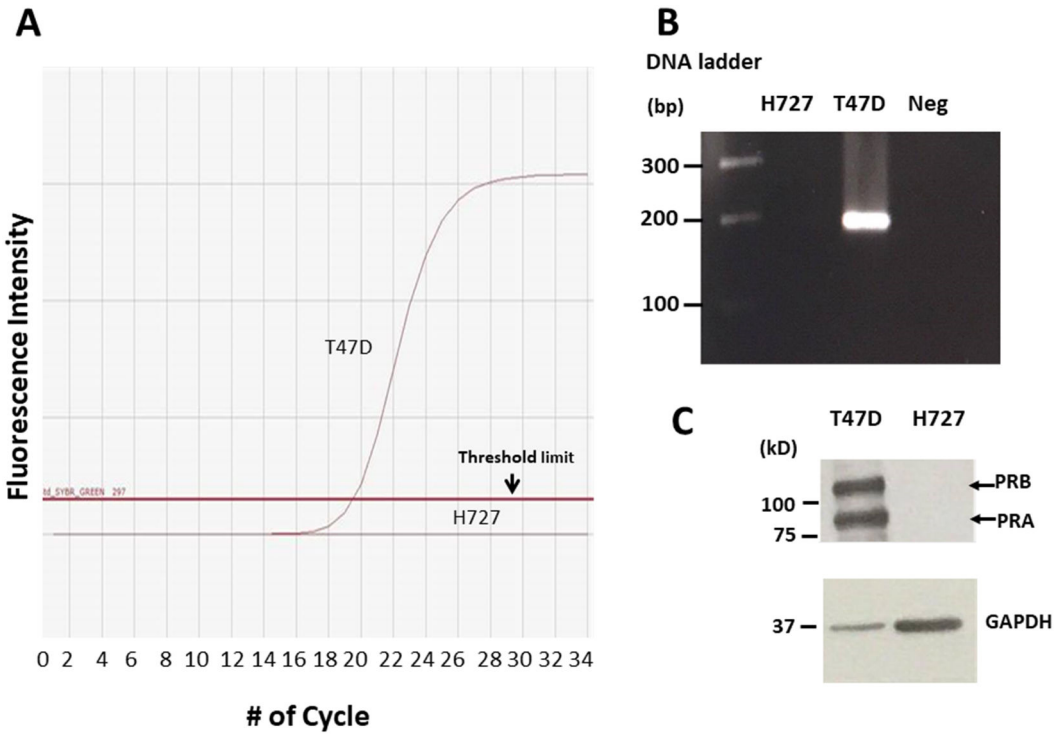

Fig 1. PR mRNA and protein expression in H727 and T47D cell lines.

(A) Total RNA was extracted from H727 and T47D cells, converted to cDNA and amplified by real time RT-PCR; results are shown as amplification plots. **(B)** Products from RT-PCR were resolved by 2% agarose gel electrophoresis: lane 1: 100 bp DNA ladder, lane 2: H727 RNA, lane 3: T47D RNA (positive control) and lane 4: no RNA template (negative control). (C) Western blot analysis were conducted with 20 μg of cell lysates from H727 cells and 3 μg of cell lysates from T47D cells using PR-specific mouse monoclonal antibody (1294 mAb). Protein loading was normalized using GAPDH as an internal control.

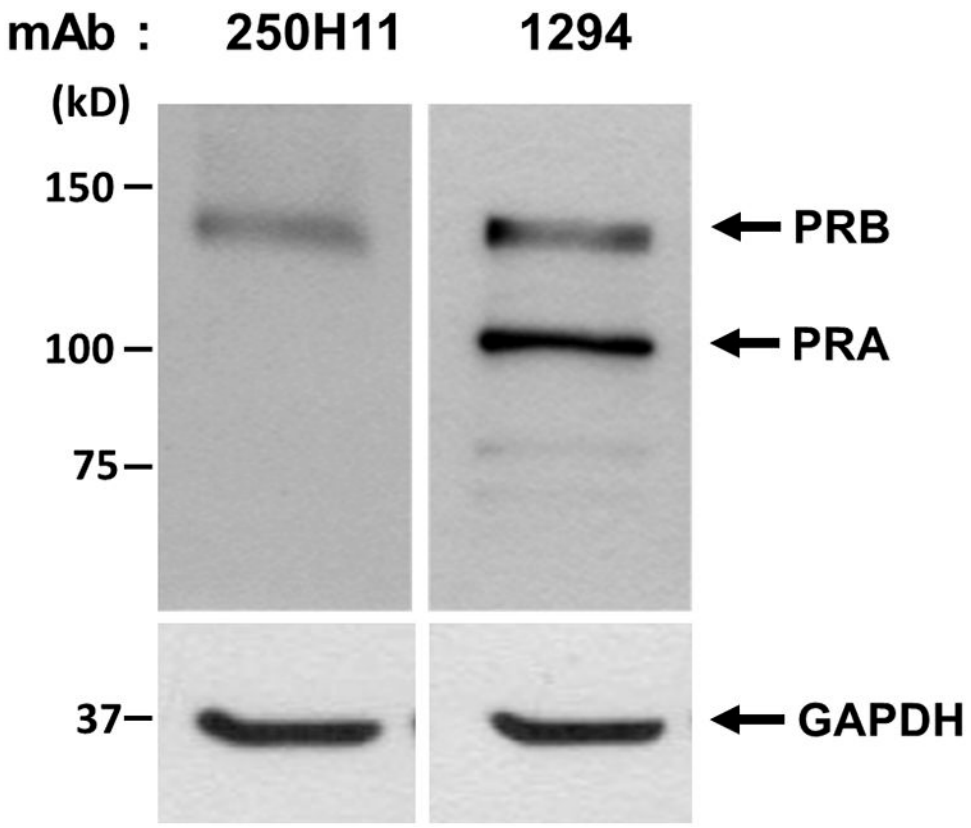

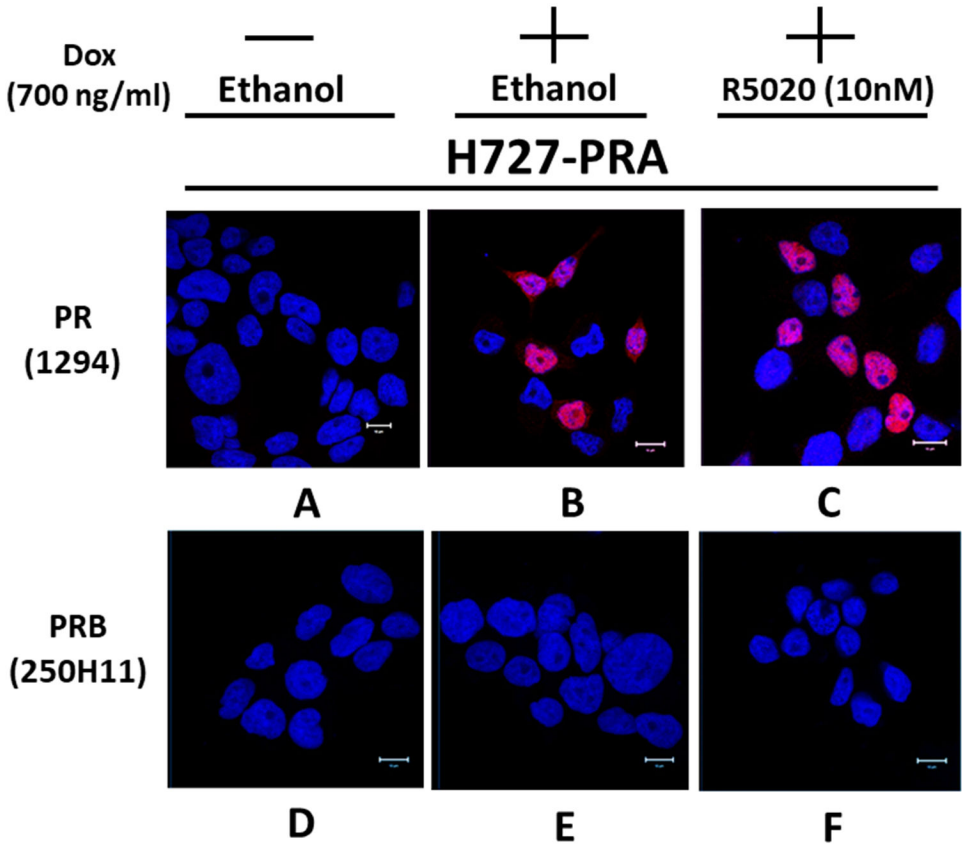

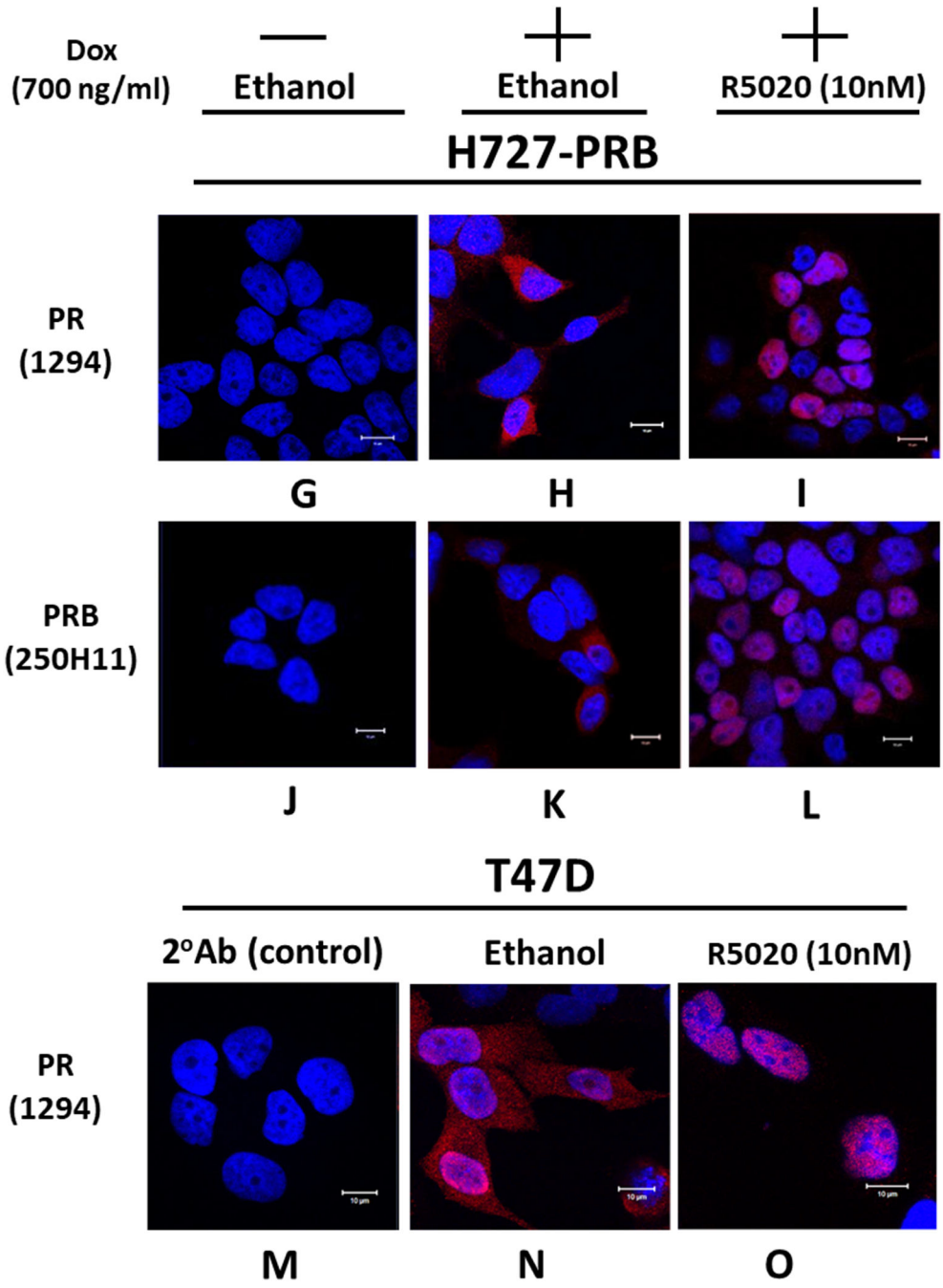

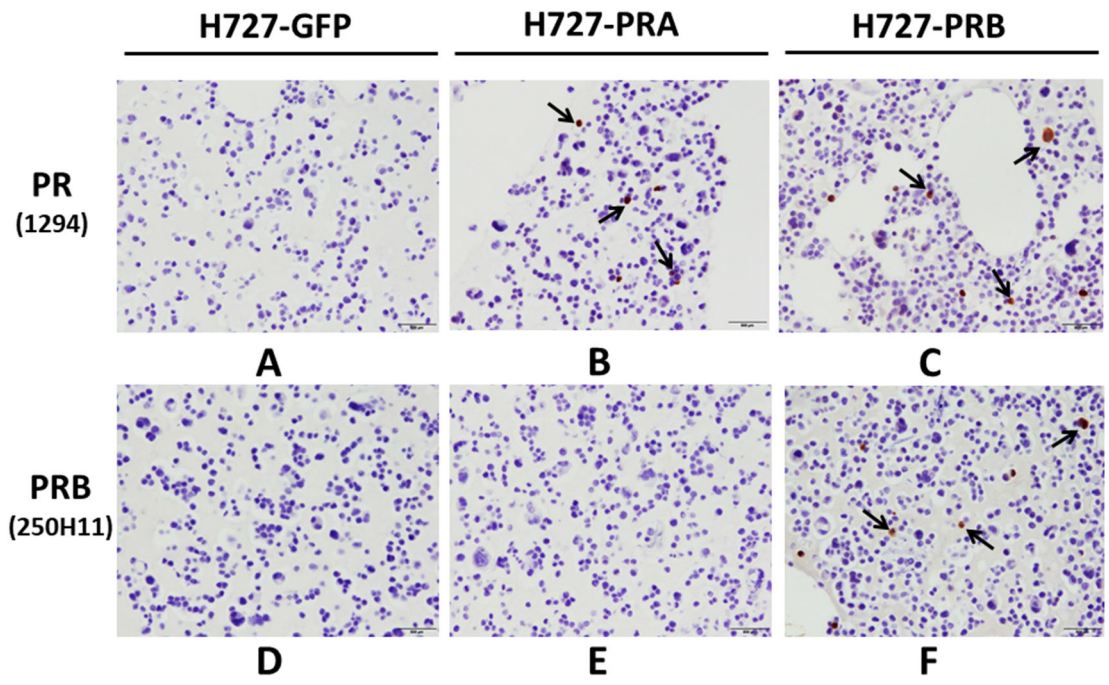

Fig 2. Characterization of the PRB-specific (250H11) monoclonal antibody by Western blot analysis and immunofluorescence.

(A) T47D cells expressing PRA and PRB were lysed and analyzed with PRB-specific mouse monoclonal antibody (250H11 mAb) and PR (PRA&PRB)-specific mAb (1294 mAb) by Western blot analysis. **(B)** H727-PRA, H727-PRB and T47D were analyzed by immunofluorescence as described in Materials and Methods. PR-specific (1294 mAb) antibody was used. Panels A and G show control untreated cells. Panels B and H respectively show H727-PRA and H727-PRB cells treated with 700 ng/ml doxycycline (Dox) for 24 hours. Panels C and I respectively show H727-PRA and H727-PRB treated with 700 ng/ml Dox for 24 hours and 10 nM R5020 for 60 min. PRB-specific (250H11) antibody was used. Panels D and J show control untreated cells. Panels E and K respectively show H727-PRA and H727-PRB cells treated with 700 ng/ml Dox for 24 hours. Panels F and L respectively show H727-PRA and H727-PRB cells treated with 700 ng/ml Dox for 24 hours and 10 nM R5020 for 60 min. T47D breast cancer cells were used as a positive control for PR expression. Panel M shows T47D cells incubated with secondary antibody alone (negative control). Panels N and O show T47D cells treated with either vehicle (Ethanol) or 10 nM R5020 for 60 min, respectively. Magnification, 1000x, Bars, 10 μm. **(C)** H727-GFP, H727-PRA and H727-PRB were treated with 700 ng/ml doxycycline (Dox) for 24 hours and stained by PR (1294) or PRB (250H11) monoclonal antibody. Panels A, B and C show treated H727-GFP, H727-PRA and H727-PRB cells, respectively, stained with PR-specific (1294 mAb) antibody. Panels D, E and F show treated H727-GFP, H727-PRA and H727-PRB cells, respectively, stained with PRB-specific (250H11) antibody.

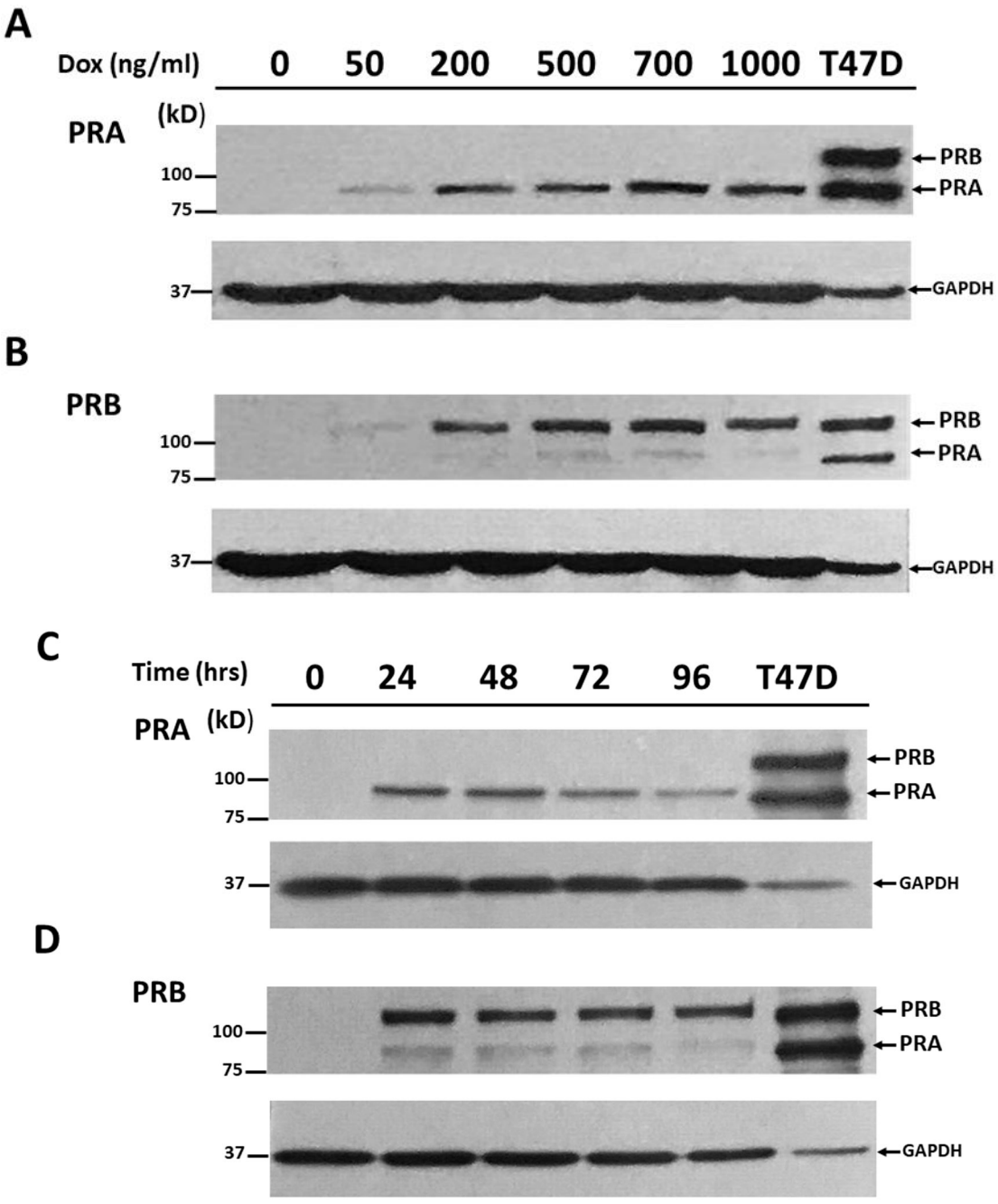

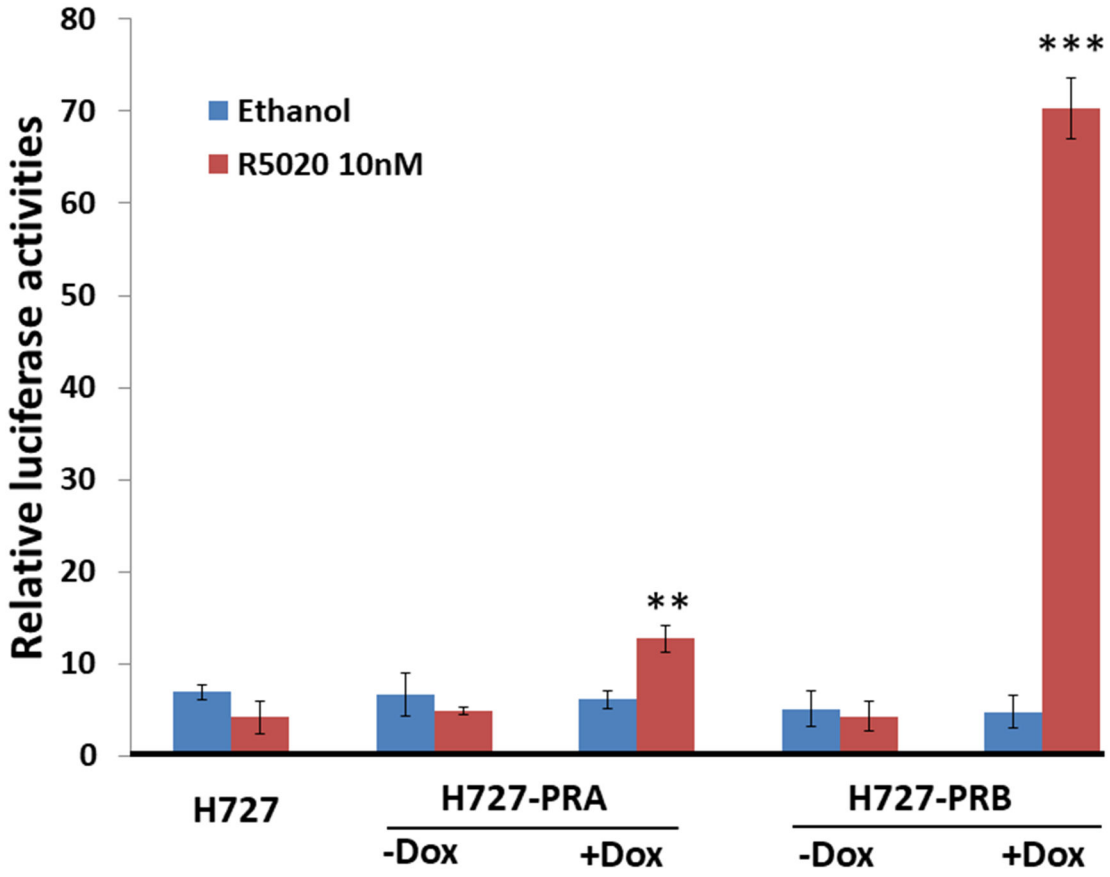

Fig 3. H727-PRA and H727-PRB cell model validation of PRA and PRB protein expression by Western blot analysis and transcriptional activities by luciferase reporter analysis.

(A) Panels A and B, H727 cells were induced to express PRA and PRB with increasing Dox concentrations (0, 50, 200, 500, 700 and 1000 ng/ml). Dox dose-dependently induced PRA and PRB protein expression in the H727-PRA and H727-PRB cell models, respectively. Panels C and D, cells were treated with the most effective dose of Dox (700 ng/ml) in a time course study (0, 24, 48, 72 and 96 hours) to induce PRA and PRB protein expression, respectively. Western blot analyses were carried out on cell lysates, and blots were stained with PR-specific antibody 1294 mAb. Thirty micrograms of protein from H727-PRA or H727-PRB cells were loaded in each lane. Two micrograms of T47D cell lysate was used as a positive control. GAPDH was used as an internal control. **(B)** Relative luciferase activities of Firefly and Renilla luciferase in H727-PRA and H727-PRB cells. Treatment with Dox and R5020 significantly increased the luciferase activities in H727-PRA and H727-PRB cells compared to cells treated with vehicle (ethanol) (*P≤0.05, **p≤0.01). Values are presented as the means ± SEM from independent experiments performed in triplicate (n=3).

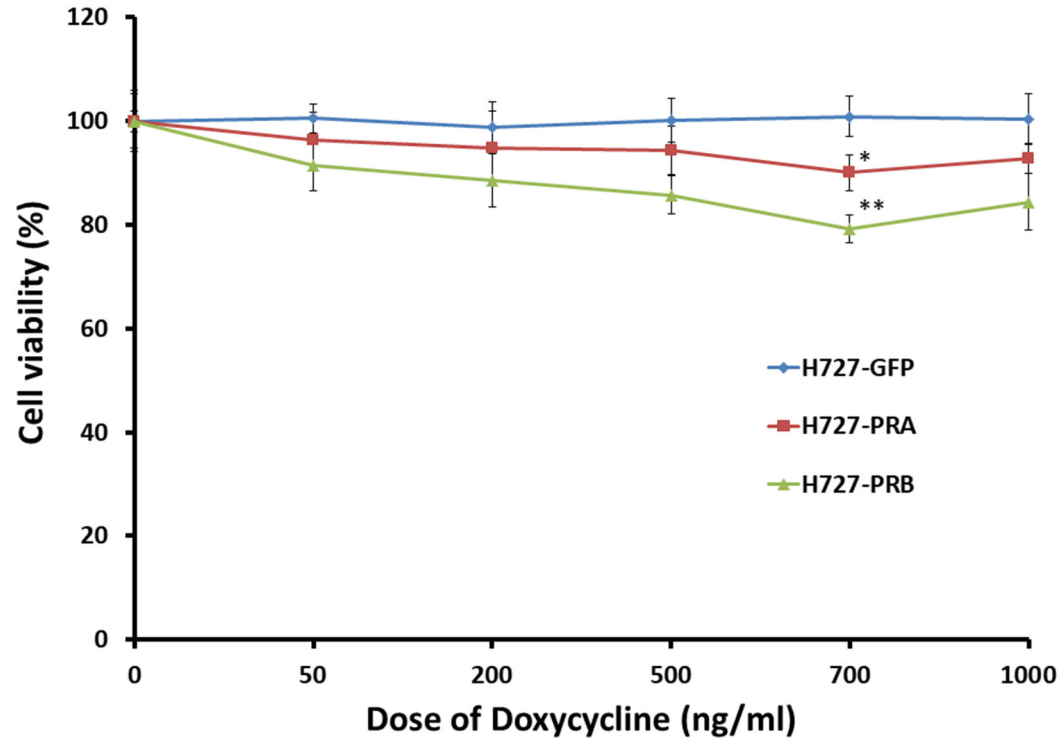

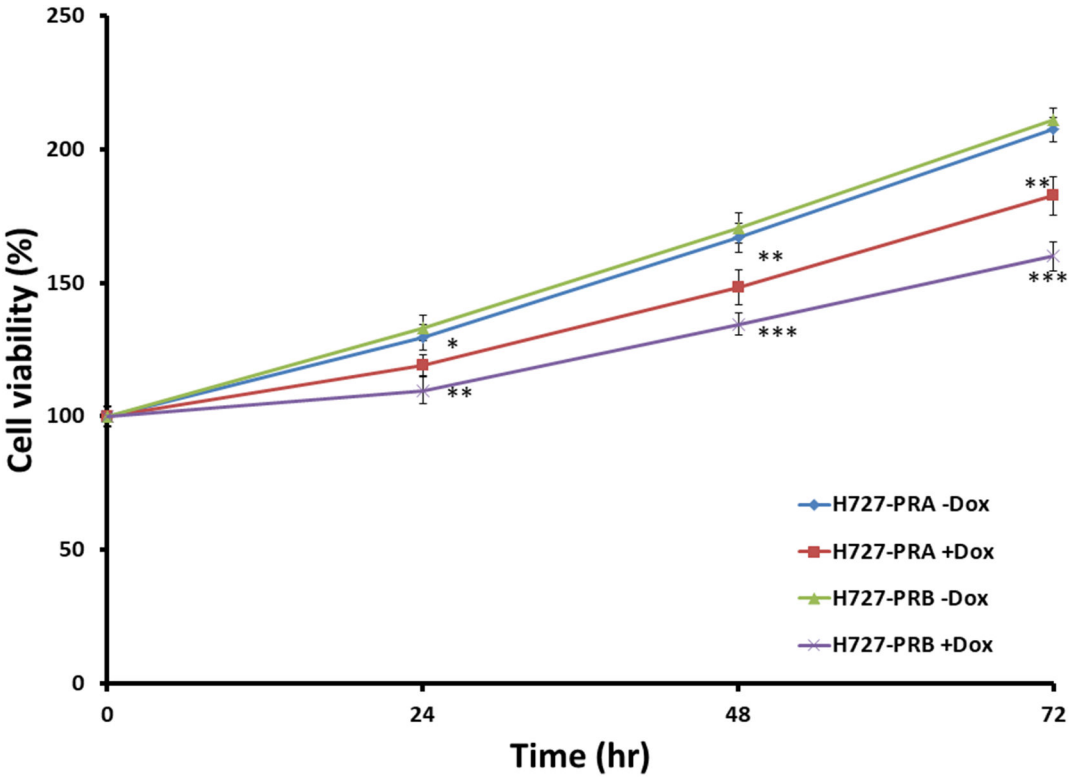

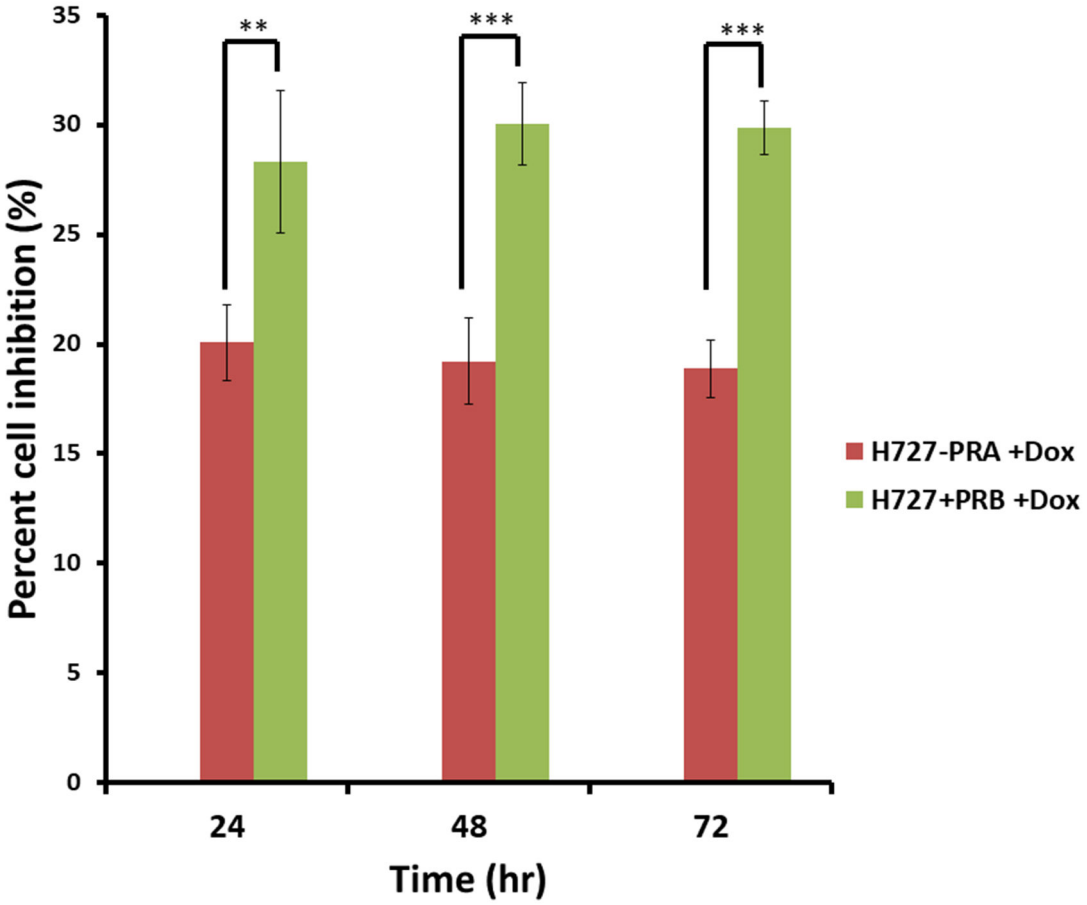

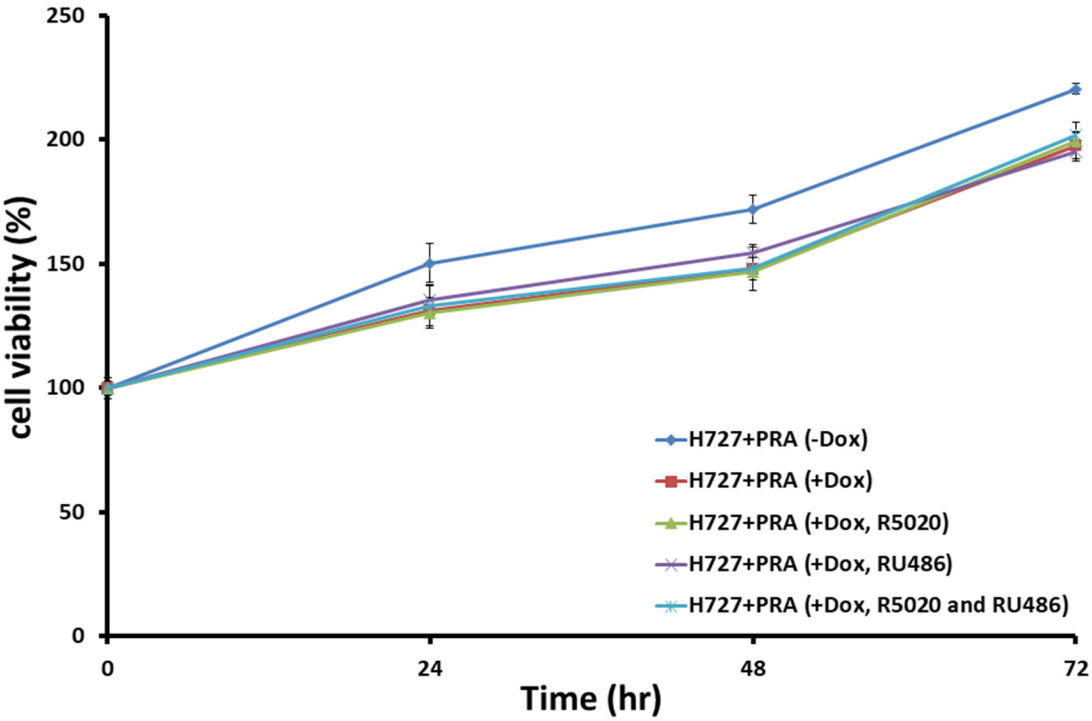

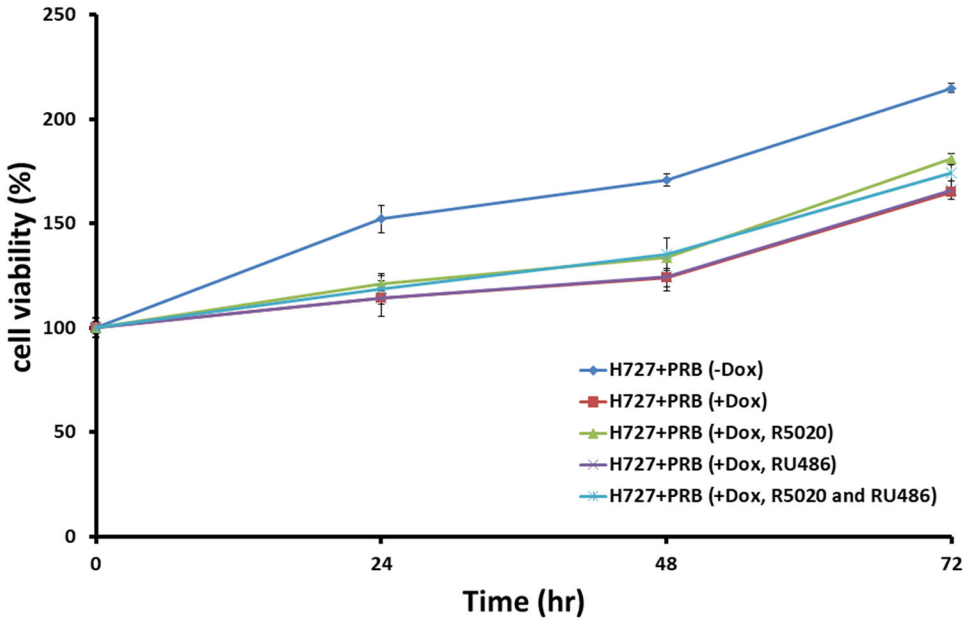

Fig 4. Effects of PRA and PRB on the absence and presence of progestin and antiprogestin in H727 lung NET cell proliferation.

(A) H727-GFP, H727-PRA and H727-PRB cells were treated with increasing concentrations of Dox (0, 50, 200, 500, 700 and 1000 ng/ml) for 48 hours and were analyzed by an MTT assay. * and ** indicate $p<0.05$ and $p<0.01$ when compared with control untreated cells, respectively. Values are presented as the means ± SEMs from independent experiments performed in triplicate (n=3). Percent cell viability represents percent cell viability of Dox-treated cells normalize to percent cell viability of control untreated cells. **(B)** H727-PRA and H727-PRB cells were treated with 700 ng/ml Dox and incubated for 24, 48 and 72 hours. ** and *** indicate $p<0.01$ and $p<0.001$ when compared with control untreated cells, respectively. Values are presented as the means ± SEMs from independent experiments performed in triplicate (n=3). **(C)** Comparison of percent inhibition of cell growth in H727-PRA and H727-PRB cells. ** indicates $p<0.01$ when compared percent cell inhibition between H727-PRB and H727-PRA cells. Values are presented as the means ± SEMs from independent experiments performed in triplicate (n=3). Percent inhibition by PRA or PRB was calculated by setting untreated control at 100% inhibition. Effects of progestin (R5020) and antiprogestin (RU486) on H727-PRA and H727-PRB cell proliferation. H727-PRA **(D)** and H727-PRB **(E)** cells were treated with 700 ng/ml Dox, 10 nM R5020, 100 nM RU486 or the combination of 10 nM R5020 and 100 mM RU486 (R5020+RU486). Cells were treated with 700 ng/ml Dox for 24 hours, and then, the medium was changed to Dox with vehicle (ethanol), R5020, RU486 or R5020+RU486 and incubated for 24 and 48 hours. X-axis values indicate time after R5020 and RU486 treatment. Values are presented as the means ± SEMs from independent experiments performed in triplicate (n=3).

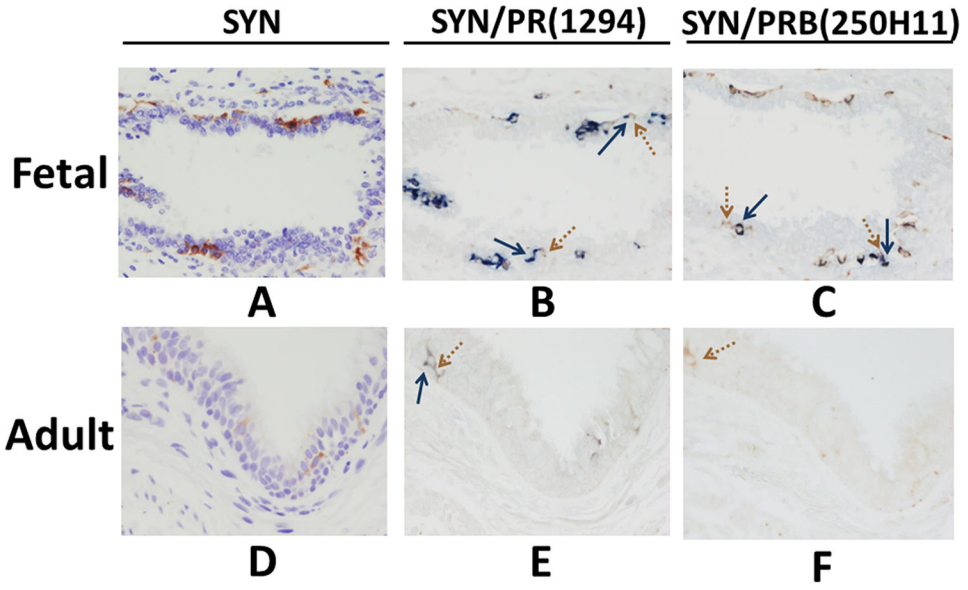

Fig 5. Double immunohistochemistry of SYN, PR and PRB in serial tissue sections of normal fetal and adult lung.

Panels A and D, tissues were stained with SYN. Panels B and E, tissues were stained with SYN (brown arrow) in combination with PR (PR, 1294 mAb, **blue arrow**), and panels C and F were staining of SYN (brown) in combination with PRB-specific antibody (250H11 mAb, blue) (magnification 400x).

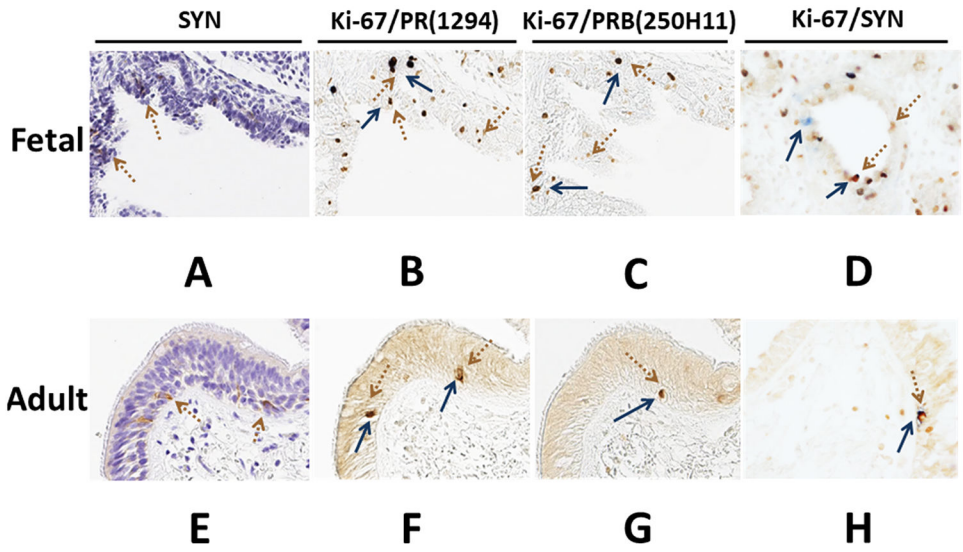

Fig 6. Double immunohistochemistry of SYN, Ki-67, PR and PRB in serial tissue sections of normal fetal and adult lung.

Panels A and D, tissues were stained with SYN. Panels B and E, tissues were stained with Ki-67 (brown arrow) in combination with PR (PR, 1294 mAb, **blue arrow**), and panels C and F were staining of Ki-67 (brown) in combination with PRB-specific antibody (250H11 mAb, blue) (magnification 400x).

Table 1.

Comparison of mean ratio between double IHC of PR and PRB with SYN and Ki-67 in normal fetal and adult lung

Normal lung	PR^+ : SYN (%)	PRB^+ : SYN (%)	p-value	PR^+ : Ki-67 (%)	PRB^+ : Ki-67 (%)	p-value
Fetal	75.86±17.21	56.05±19.78	0.038*	57.64±7.71	41.27±7.91	<0.001*
Adult	56.62±26.12	32.54±18.31	0.029*	91.53±7.34	57.37±13.02	<0.001*

PR^+: SYN^+ = Ratio in percent of PR positive cells with SYN positive cells in double immunohistochemistry staining

PRB^+: SYN^+ = Ratio in percent of PRB positive cells with SYN positive cells in double immunohistochemistry staining

PR^+: Ki-67^+ = Ratio in percent of PR positive cells with Ki-67 positive cells in double immunohistochemistry staining

PRB^+: Ki-67^+ = Ratio in percent of PRB positive cells with Ki-67 positive cells in double immunohistochemistry staining

Table 2.

Comparison of mean ratio double IHC of PR and PRB with SYN and Ki-67 between normal fetal and adult lung

Ratio	Normal lung		p-value
	Fetal	Adult	
PR+ : SYN (%)	75.86±17.21	56.62±26.12	0.079
PRB+ : SYN (%)	56.05±19.78	32.54±18.31	0.016*
PR+ : Ki-67 (%)	57.64±7.71	91.53±7.34	<0.001*
PRB+ : Ki-67 (%)	41.27±7.91	57.37±13.02	0.005*
Ki-67 : SYN (%)	67.87±16.76	72.43±15.99	0.552

PR^+: SYN^+ = Ratio in percent of PR positive cells to SYN positive cells in double immunohistochemistry staining

PRB^+: SYN^+ = Ratio in percent of PRB positive cells with SYN positive cells in double immunohistochemistry staining

PR^+: $Ki\text{-}67^+$ = Ratio in percent of PR positive cells with Ki-67 positive cells in double immunohistochemistry staining

PRB^+: $Ki\text{-}67^+$ = Ratio in percent of PRB positive cells with Ki-67 positive cells in double immunohistochemistry staining

$Ki\text{-}67^+$: SYN^+ = Ratio in percent of Ki-67 positive cells with SYN positive cells in double immunohistochemistry staining